Increased Th17-Inducing Activity of CD14$^+$ CD163^{low} Myeloid Cells in Intestinal Lamina Propria of Patients With Crohn's Disease

TAKAYUKI OGINO,[1] JUNICHI NISHIMURA,[1] SOUMIK BARMAN,[2,3] HISAKO KAYAMA,[2,3] SATOSHI UEMATSU,[4] DAISUKE OKUZAKI,[5] HIDEKI OSAWA,[1] NAOTSUGU HARAGUCHI,[1] MAMORU UEMURA,[1] TAISHI HATA,[1] ICHIRO TAKEMASA,[1] TSUNEKAZU MIZUSHIMA,[1] HIROFUMI YAMAMOTO,[1] KIYOSHI TAKEDA,[2,3,6] YUICHIRO DOKI,[1] and MASAKI MORI[1]

[1]Department of Gastroenterological Surgery, [2]Laboratory of Immune Regulation, Graduate School of Medicine, Osaka University, Osaka, Japan; [3]Laboratory of Mucosal Immunology, Immunology Frontier Research Center, Osaka University, Osaka, Japan; [4]Division of Innate Immune Regulation, International Research and Development Center for Mucosal Vaccines, Institute of Medical Science, Tokyo University, Tokyo, Japan; [5]DNA-Chip Developemental Center for Infectious Diseases, Research Institute for Microbial Diseases, Osaka University, Osaka, Japan; and [6]Core Research for Evolutional Science and Technology, Japan Science and Technology Agency, Saitama, Japan

BACKGROUND & AIMS: Abnormal activity of innate immune cells and T-helper (Th) 17 cells has been implicated in the pathogenesis of autoimmune and inflammatory diseases, including Crohn's disease (CD). Intestinal innate immune (myeloid) cells have been found to induce development of Th17 cells in mice, but it is not clear if this occurs in humans or in patients with CD. We investigated whether human intestinal lamina propria cells (LPCs) induce development of Th17 cells and whether these have a role in the pathogenesis of CD. **METHODS:** Normal intestinal mucosa samples were collected from patients with colorectal cancer and noninflamed and inflamed regions of mucosa were collected from patients with CD. LPCs were isolated by enzymatic digestion and analyzed for expression of HLA-DR, lineage markers CD14 and CD163 using flow cytometry. **RESULTS:** Among HLA-DR^{high} Lin$^-$ cells, we identified a subset of CD14$^+$ CD163^{low} cells in intestinal LPCs; this subset expressed Toll-like receptor (*TLR*) *2*, *TLR4*, and *TLR5* mRNAs and produced interleukin (IL)-6, IL-1β, and tumor necrosis factor in response to lipopolysaccharide. In vitro co-culture with naïve T cells revealed that CD14$^+$ CD163^{low} cells induced development of Th17 cells. CD14$^+$ CD163^{low} cells from inflamed regions of mucosa of patients with CD expressed high levels of *IL-6*, *IL-23p19*, and tumor necrosis factor mRNAs, and strongly induced Th17 cells. CD14$^+$ CD163^{low} cells from the noninflamed mucosa of patients with CD also had increased abilities to induce Th17 cells compared with those from normal intestinal mucosa. **CONCLUSIONS: CD14$^+$ CD163^{low} cells in intestinal LPCs from normal intestinal mucosa induce differentiation of naive T cells into Th17 cells; this activity is increased in mucosal samples from patients with CD. These findings show how intestinal myeloid cell types could contribute to pathogenesis of CD and possibly other Th17-associated diseases.**

Keywords: Dendritic Cell; Macrophage; Helper T Cell; Inflammatory Bowel Disease.

Recent studies have suggested that innate immune cells, including macrophages and dendritic cells (DC) of the intestinal mucosa, play important roles in maintaining gut homeostasis by protecting the host from foreign pathogens and by negatively regulating excess immune responses to commensal bacteria and dietary antigens.[1,2] Inappropriate immune reactions to commensal bacteria can lead to development of inflammatory bowel diseases (IBD), such as Crohn's disease (CD) and ulcerative colitis.[3,4] The identification of interleukin (IL)-17–producing Th17 cells offers new insight into the induction and regulation of mucosal immunity, which is linked to IBD pathogenesis.[5–7] Additionally, genome-wide association studies have shown significant associations of CD with Th17-related inflammatory pathways and innate microorganism sensors.[8–13]

Several subsets of murine intestinal innate immune cells have been found to modulate intestinal homeostasis.[14] In the CD11c$^+$ cell subset, CD103$^+$ and CX3CR1$^+$ cells represent nonoverlapping populations with different precursors.[15–17] CD103$^+$ cells uptake luminal antigens in the lamina propria by a unique mechanism, move to the mesenteric lymph nodes (MLN), and activate T cells.[18,19] They can induce expression of gut homing receptors (CCR9 and $\alpha4\beta7$ integrin) on T cells, activate CD8$^+$ T cells, and induce differentiation of Foxp3-expressing regulatory T cells.[20–22] CX3CR1$^+$ cells can be divided into 2 subsets based on CX3CR1 expression level: CX3CR1^{int} and CX3CR1^{high} cells.[15,23] CX3CR1^{int} cells are DCs that induce Th17 cells and migrate into the inflammatory regions,[23–28] and CX3CR1^{high} cells possess anti-inflammatory properties and inhibit T-cell responses.[26,29,30] These findings strongly support the notion that intestinal innate immune cells regulate gut homeostasis.

Compared with murine intestinal innate immune cells, human intestinal cells remain less well characterized. It

Abbreviations used in this paper: CD, Crohn's disease; CDi, inflamed region of CD; CDn, noninflamed region of CD; DC, dendritic cell; IBD, inflammatory bowel disease; IFN, interferon; IL, interleukin; int, intermediate; LPC, lamina propria cell; MLN, mesenteric lymph node; mRNA, messenger RNA; NC, normal colon from colon cancer patients; slan, 6-sulfo LacNAc; TGF, transforming growth factor; Th, T-helper; TLR, Toll-like receptor; TNF, tumor necrosis factor.

0016-5085/$36.00
http://dx.doi.org/10.1053/j.gastro.2013.08.049

has been reported that resident intestinal macrophages fail to produce proinflammatory cytokines in response to Toll-like receptor (TLR) ligands, in spite of active phagocytic and bactericidal activities.[31,32] A unique subset of macrophages that express macrophage (CD14, CD33, CD68) and DC (CD205, CD209) markers reportedly contributes to IBD pathogenesis through induction of IL-23–dependent interferon (IFN) gamma responses by T cells, as well as potent antigen-presenting activity.[33,34] Similar to the mouse intestinal $CD103^+$ cells, $CD103^+$ DCs that can induce gut homing receptors have been identified in the human small intestine.[20] However, human intestinal lamina propria cells (LPCs) equivalent to mouse $CX3CR1^+$ cells have not yet been characterized. Most recently, human LPCs have been classified into subsets based on the expressions of CD14, HLA-DR, CD209, CD163, and CD11c.[28] However, functional characterization of these human LPC subsets remains elusive.

In the present study, we show that $HLA\text{-}DR^{high}$ Lin^- cells in human intestinal lamina propria comprise 4 subsets that are distinguished by differential expression patterns of CD14, CD11c, and CD163. We further show that $HLA\text{-}DR^{high}$ Lin^- $CD14^+$ $CD163^{low}$ cells induce Th17 cell differentiation. CD patients exhibited exceedingly enhanced Th17 immunity induced by $HLA\text{-}DR^{high}$ Lin^- $CD14^+$ $CD163^{low}$ cells, even in noninflamed intestine.

Methods

Tissue Samples

Normal intestinal mucosa was obtained from microscopically and macroscopically intact areas in patients with colorectal cancer. Intestinal mucosa was also obtained from surgically resected specimens from patients with CD who were diagnosed based on established clinical, bacteriological, radiologic, and endoscopic criteria. Histopathological analysis showed moderate to severe inflammation in all samples from patients with CD. This study was approved by the Ethical Committee of Osaka University School of Medicine and informed consent for specimen use was obtained from all patients.

Isolation of LPCs

To isolate LPCs, intestinal mucosa was washed in phosphate-buffered saline to remove feces. Then, intestinal mucosa was placed in RPMI 1640 containing 5 mM EDTA and incubated for 10 minutes in a 37°C shaking water bath. After washing in phosphate-buffered saline, the mucosa was cut into small pieces and incubated in RPMI 1640 containing 10% fetal bovine serum, 2 mg/mL collagenase D (Roche, Basel, Switzerland), 1 mg/mL dispase (Invitrogen, Carlsbad, CA), and 15 μg/mL DNase I (Roche) for 60 minutes in a 37°C shaking water bath. The digested tissues were then passed through a 40-μm cell strainer. The isolated cells were washed with RPMI 1640 containing 5 mM EDTA, resuspended in 5 mL 20% Percoll (GE Healthcare Japan, Tokyo, Japan), and then overlaid on 2.5 mL 40% Percoll in a 15-mL tube. Percoll gradient separation was performed by centrifugation at 500*g* for 30 min at 4°C. The LPCs were collected from the interface of the Percoll gradient, then washed twice with phosphate-buffered saline containing 2% fetal bovine serum.

Flow Cytometry

The antibodies for flow cytometry are shown in the Supplementary Material. Flow cytometric analysis was performed using a FACSCantoII flow cytometer (BD Biosciences, San Jose, CA). LPCs were purified using a FACSAriaII system (BD Biosciences), and data were analyzed with FlowJo software (Tree Star, Ashland, OR).

Morphological Analysis

Isolated LPC subsets were spread on glass slides and were air dried. The spread cells were fixed with methanol, stained by May-Grünwald-Giemsa method, and observed with a microscope (BZ-9000; KEYENCE, Itasca, IL).

Microarray Analysis

Total RNA derived from LPCs was reverse transcribed by using an Ovation Pico WTA System V2 (NuGen, San Carlos, CA) and labeled with cyanine-3 using a Genomic DNA Enzymatic Labeling Kit (Agilent Technologies, Santa Clara, CA). The labeled complementary DNA was hybridized to SurePrint G3 Human Gene Expression v2 8x60K Microarray (G4845A) (Agilent Technologies). The data have been deposited in GEO as GSE49066. See the Supplemental Material for more details.

Quantitative Real-Time Reverse Transcription Polymerase Chain Reaction

Total RNA was isolated using the RNeasy Mini kit (Qiagen, Valencia, CA). RNA was reverse-transcribed using Moloney murine leukemia virus reverse transcriptase (Promega, Madison, WI) and random primers (TOYOBO, Osaka, Japan) after treatment with RQ1DNase I (Promega). Quantitative real-time polymerase chain reaction was performed on a Light Cycler 2.0 (Roche) with the TaqMan Universal PCR Master Mix (Applied Biosystems, Carlsbad, CA). Amplification conditions were 95°C for 10 minutes, then 45 cycles of 95°C for 10 seconds, and 60°C for 30 seconds. All data were normalized to the expression of the glyceraldehyde 3-phosphate dehydrogenase gene. The primer sets and probes are shown in Supplementary Table 1.

Cytokine Assay

LPCs were cultured with 1 μg/mL FSL-1 (Invivogen), 1 μg/mL LPS (Sigma, St Louis, MO), or 1 μg/mL flagellin (Invivogen) for 72 hours at 37°C. The culture supernatants were collected and enzyme-linked immunosorbent assay was performed with the Human Th1/Th2 11plex FlowCytomix kit (eBioscience, San Diego, CA).

In Vitro T-Cell Differentiation

Allogeneic naive $CD4^+$ T cells were co-cultured at 37°C with the indicated cells at a ratio of 1:5 in the presence of 10 U/mL IL-2 (Roche), 2 μg/mL anti-CD3 (BD Biosciences), and 5 μg/mL anti-CD28 (BD Biosciences). After 5 days, cells were analyzed by fluorescence-activated cell sorting. In cytokine blocking experiments, cells were cultured in the presence of 2.5 μg/mL anti–transforming growth factor (TGF)–β, 2.5 μg/mL

anti–IL-1β, 2.5 μg/mL anti–IL-6, or 0.5 μg/mL anti–IL-23 (R&D Systems, Minneapolis, MN).

Statistical Analysis

Differences between the control and experimental groups were evaluated using the Student's *t* test. Statistical analyses were performed using JMP version 9.02 (SAS Institute, Cary, NC). *P* values < .01 were considered statistically significant.

Results

Phenotypic Characterization of Human Colonic LPC Subsets

We used a combination of surface markers to characterize LPC subsets in noninvaded colonic tissue samples from colorectal cancer patients. After LPC isolation from colonic tissues, single-cell suspensions were analyzed for expression of lineage markers (CD3, CD19, CD20, and CD56), HLA-DR, CD14, CD11c, and CD163 (Figure 1*A*). To characterize LPCs that were involved in mediating T-cell differentiation and activation, we focused on HLA-DR^{high} cells. HLA-DR^{high} Lin$^-$ cells comprised 3.7%–5.1% of total LPCs, and were divided into 3 subsets: CD14$^-$ CD11c^{low}, CD14$^-$ CD11c^{high}, and CD14$^+$ CD11c$^+$ cells. CD14$^-$ CD11c^{low} and CD14$^-$ CD11c^{high} cells each did not express CD163 (data not shown), and CD14$^+$ CD11c$^+$ cells were further subdivided into 2 populations: CD163^{low} CD14$^+$ CD11c$^+$ and CD163^{high} CD14$^+$ CD11c$^+$ cells; hereafter, these cells are designated CD14$^+$ CD163^{low} and CD14$^+$ CD163^{high} cells, respectively. In total, human colonic HLA-DR^{high} Lin$^-$ cells comprised 4 subsets: CD14$^+$ CD163^{low} (24.7% ± 8.2% of all HLA-DR^{high} Lin$^-$ cells), CD14$^+$ CD163^{high} (14.7% ± 4.7%), CD14$^-$ CD11c^{high} (18.8% ± 7.9%), and CD14$^-$ CD11c^{low} (30.3% ± 8.9%) cells (Figure 1*B*). CD14$^+$ CD163^{low} and CD14$^+$ CD163^{high} cells showed macrophage-like morphologies with numerous cytoplasmic vacuoles (Figure 1*C*).

We then analyzed whether these populations were present in other tissues (Figure 1*D*). In the small intestinal

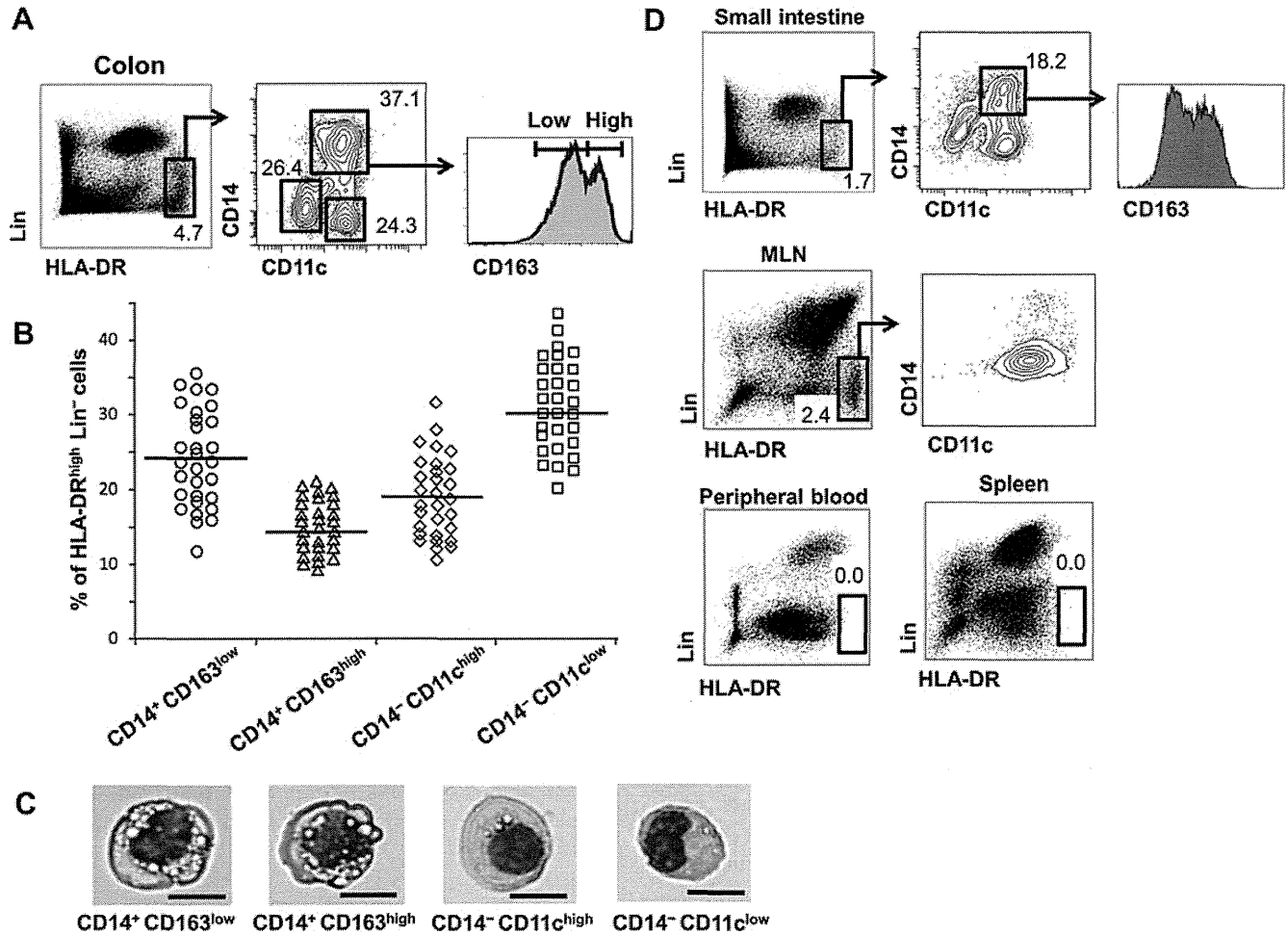

Figure 1. Characterization of LPC subsets. (*A*) Flow cytometry analysis of LPCs from normal intestine of colorectal cancer patients. Live HLA-DR^{high} Lin$^-$ cells were gated and analyzed for expression of CD14 vs CD11c (Lin; CD3, CD19, CD20, CD56). Three populations were defined (CD14$^-$ CD11c$^-$, CD14$^-$ CD11c$^+$, and CD14$^+$ CD11c$^+$), and the CD14$^+$ CD11c$^+$ population was further analyzed for CD163 expression. Representative results of 30 independent experiments are shown. (*B*) Percentages of LPC subsets among HLA-DR^{high} Lin$^-$ cells of 30 patients; *horizontal bars* indicate mean. (*C*) Morphological analysis of LPC subsets by May-Grünwald-Giemsa staining. Scale bars = 10 μm. (*D*) Characterization of cell subsets from human small intestine, MLN, peripheral blood, and spleen. Representative results of 10 independent experiments are shown. *Numbers* indicate the percentage of cells in indicated gates. *Arrows* show gating strategy.

lamina propria, we observed the same 4 populations, albeit with slightly different proportions: $CD14^+$ $CD163^{low}$ (11.7% ± 4.3% of all HLA-DR^{high} Lin^- cells), $CD14^+$ $CD163^{high}$ (9.9% ± 4.1%), $CD14^-$ $CD11c^{high}$ (35.1% ± 17.2%), and $CD14^-$ $CD11c^{low}$ (33.2% ± 11.1%) cells. In the MLN, we found only small numbers of $CD14^+$ cells and increased numbers of $CD14^-$ $CD11c^{high}$ cells. HLA-DR^{high} Lin^- cells were not present in peripheral blood and spleen.

Next, we analyzed the surface expressions of several markers on these 4 subsets of human intestinal LPCs (Figure 2). $CD14^+$ $CD163^{low}$ and $CD14^+$ $CD163^{high}$ cells expressed several macrophage and DC markers, including molecules expressed on macrophages (CD16 and CD64), on DCs (CD1c, CD141, CD209, and 6-sulfo LacNAc [slan]), on both macrophages and DCs (CD11b, CD172a, and CD206), and on mature DCs (CD80, CD83, and CD86). These 2 cell subpopulations showed almost the same expression patterns for all examined surface molecules, indicating that CD163 is a unique marker that can distinguish $CD14^+$ cells subpopulations. $CD14^-$ $CD11c^{high}$ cells exhibited high expression of CD1c and CD172a as well as moderate expression of DC maturation markers, but were still heterogeneous because these cells included $CD103^+$ and $CD103^-$ populations. $CD14^-$ $CD11c^{low}$ cells were also heterogeneous, including $CD141^{high}$ and $CD141^-$ populations.

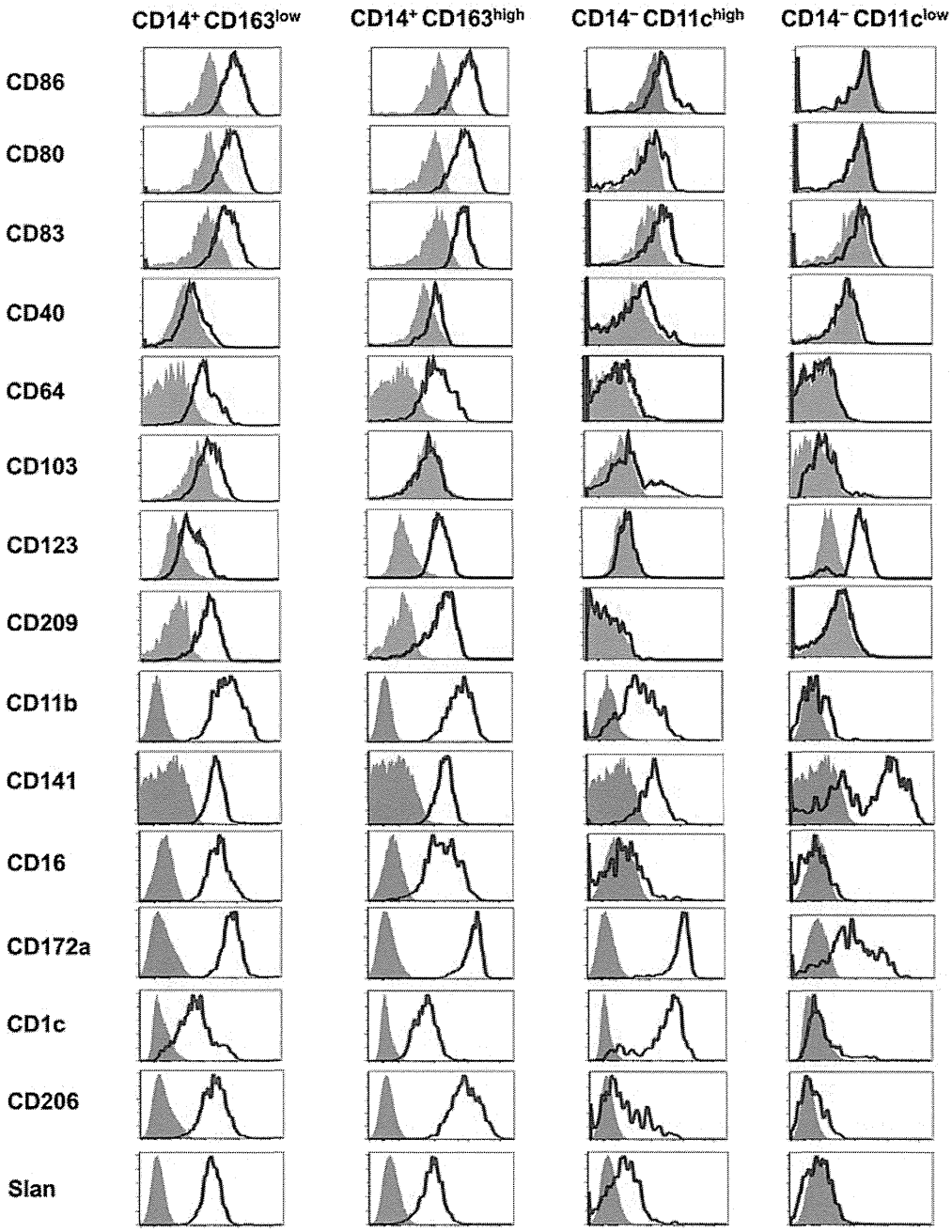

Figure 2. Phenotypic analysis of LPC subsets. Flow cytometry for surface expressions of CD86, CD80, CD83, CD40, CD64, CD103, CD123, CD209, CD11b, CD141, CD16, CD172a, CD1c, CD206, and slan in LPC subsets. The histogram shows the profiles of the indicated antibody staining, and the *shaded* histogram shows staining with isotype control. Representative results of 5–11 independent experiments are shown.

Gene Expression Features of LPC Subsets

We performed microarray analysis to compare gene expression profiles among these subsets purified from normal colon of 10 colon cancer patients. To assess the reliability of the microarray analysis, we compared expression of mRNAs encoding glyceraldehyde 3-phosphate dehydrogenase, CD163, CD14, and CD11c across LPC subsets analyzed (Supplementary Figure 1). We found that mRNA expression of these genes correlated with the surface phenotype of each subset. Hierarchical clustering of about 15,000 protein-coding genes with >2-fold change in expression in at least 1 of the 6 pairwise comparisons showed that $CD14^+$ $CD163^{low}$ cells were more closely related to $CD14^+$ $CD163^{high}$ cells than to other subsets (Figure 3*A*). When we selected genes corresponding to the DC-related and monocyte/macrophage-related biological processes (antigen processing and presentation [GO 0019882], phagocytosis [GO 0006909], monocyte differentiation [GO 0030224], or macrophage differentiation [GO 0030225]), the transcriptomic pathways of $CD14^+$ $CD163^{low}$ cells were found to be similar to those of $CD14^+$ $CD163^{high}$ cells. However, when focusing on inflammatory response to antigenic stimulus (GO 0002437), $CD14^+$ $CD163^{low}$ cells were close to $CD14^-$ $CD11c^{high}$ cells (Figure 3*B* and Supplementary Table 2). To gain more insight into the nature of LPC subsets, we analyzed expression of transcription factors and growth factor receptor, which are involved in function and development of DCs and macrophages (Supplementary Figure 2). Expression of mRNAs encoding *MAFB* and *CSFR1* (involved in macrophage differentiation) was high in $CD14^+$ $CD163^{low}$ and $CD14^+$ $CD163^{high}$ cells. $CD14^-$ $CD11c^{high}$ cells expressed the highest level of mRNAs encoding *IRF4* and *FLT3*, which are both involved in the

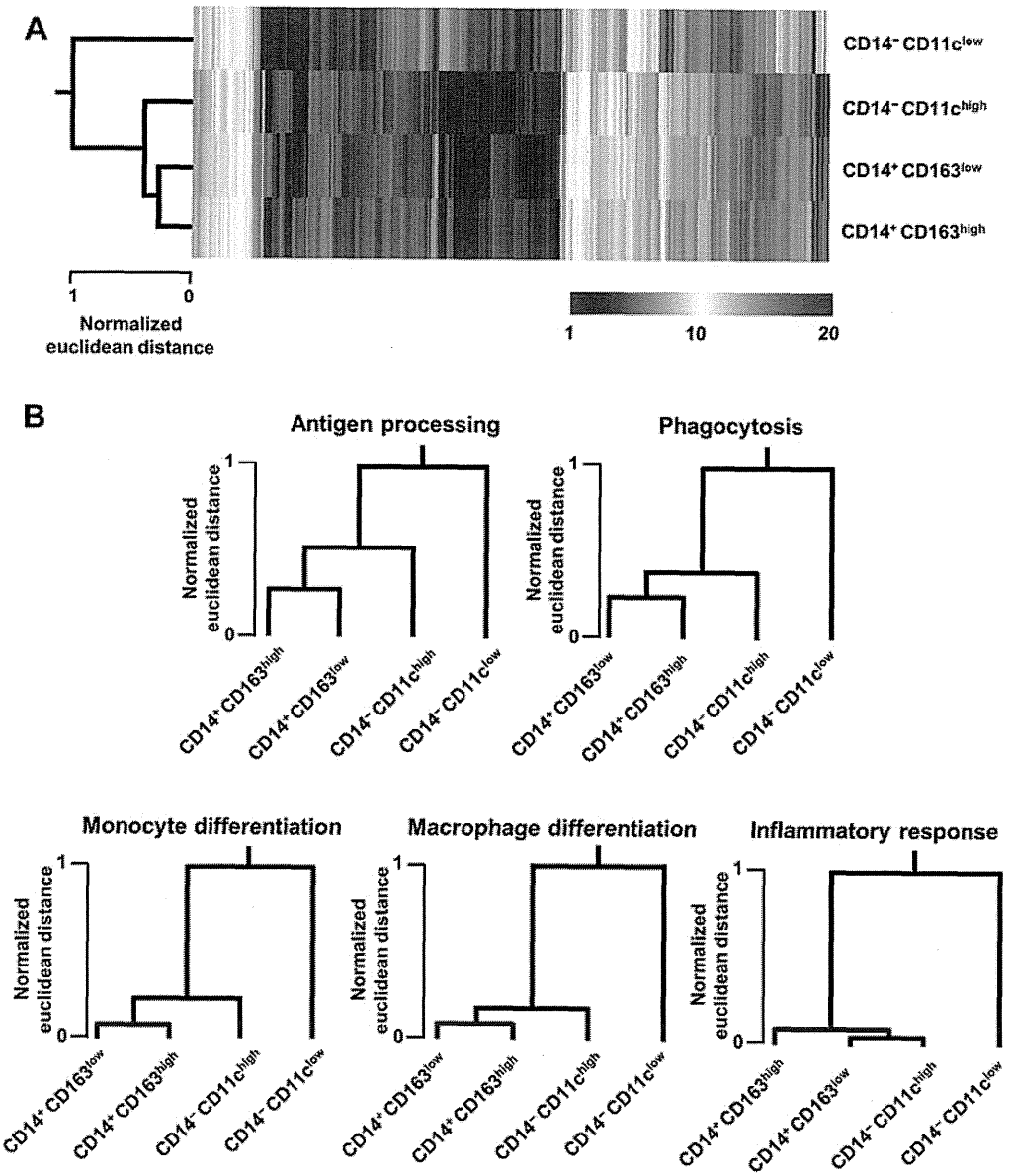

Figure 3. Gene expression profiles of LPC subsets. (*A*) Hierarchical clustering and heat map of LPC subsets was generated from about 15,000 protein-coding genes called detected in at least a subset, with >2-fold change in expression in at least 1 of the 6 possible pairwise comparisons. Euclidian distances are divided by the maximum to scale from 0 to 1. (*B*) Hierarchical clustering using sets of differentially expressed genes corresponding to the Gene Ontology biological functions of antigen processing and presentation (203 genes), phagocytosis (66 genes), monocyte differentiation (16 genes), macrophage differentiation (13 genes), or inflammatory response to antigenic stimulus (15 genes). Clustered heat maps were produced by using Euclidean distance. Euclidian distances are divided by the maximum to scale from 0 to 1.

DC differentiation process. $CD14^+$ $CD163^{low}$ cells showed higher levels of *IRF4* and *FLT3* expression than $CD14^+$ $CD163^{high}$ cells. Taken together, these results suggest that $CD14^+$ $CD163^{low}$ cells are closely related to $CD14^+$ $CD163^{high}$ cells and that the developmental pathway of $CD14^+$ $CD163^{low}$ cells have characteristics of both DC and macrophage development.

We next determined the *TLR* mRNA expression of these 4 subsets by quantitative real-time reverse transcription polymerase chain reaction (Figure 4*A*). $CD14^+$ $CD163^{low}$ cells expressed *TLR2* and *TLR4*, $CD14^+$ $CD163^{low}$, and $CD14^+$ $CD163^{high}$ cells expressed *TLR5*, and $CD14^-$ $CD11c^{high}$ cells expressed *TLR9*. $CD14^-$ $CD11c^{low}$ cells did not express any *TLR*. We also examined the gene expressions of several inflammatory and anti-inflammatory mediators (Figure 4*B*). $CD14^+$ $CD163^{low}$ cells exhibited the highest expressions of *IL-6* and *IL-23p19*. $CD14^+$ $CD163^{high}$ cells uniquely expressed several anti-inflammatory markers, including *IL-10, HMOX1,* and *TGFB*. $CD14^-$ $CD11c^{high}$ cells expressed the highest level of *IFNG* among the 4 subsets. *IL-12p35* expression was observed only in $CD14^-$ $CD11c^{low}$ cells. Overall, the 4 subsets of intestinal LPCs showed differential expression patterns of inflammatory genes, and the $CD14^+$

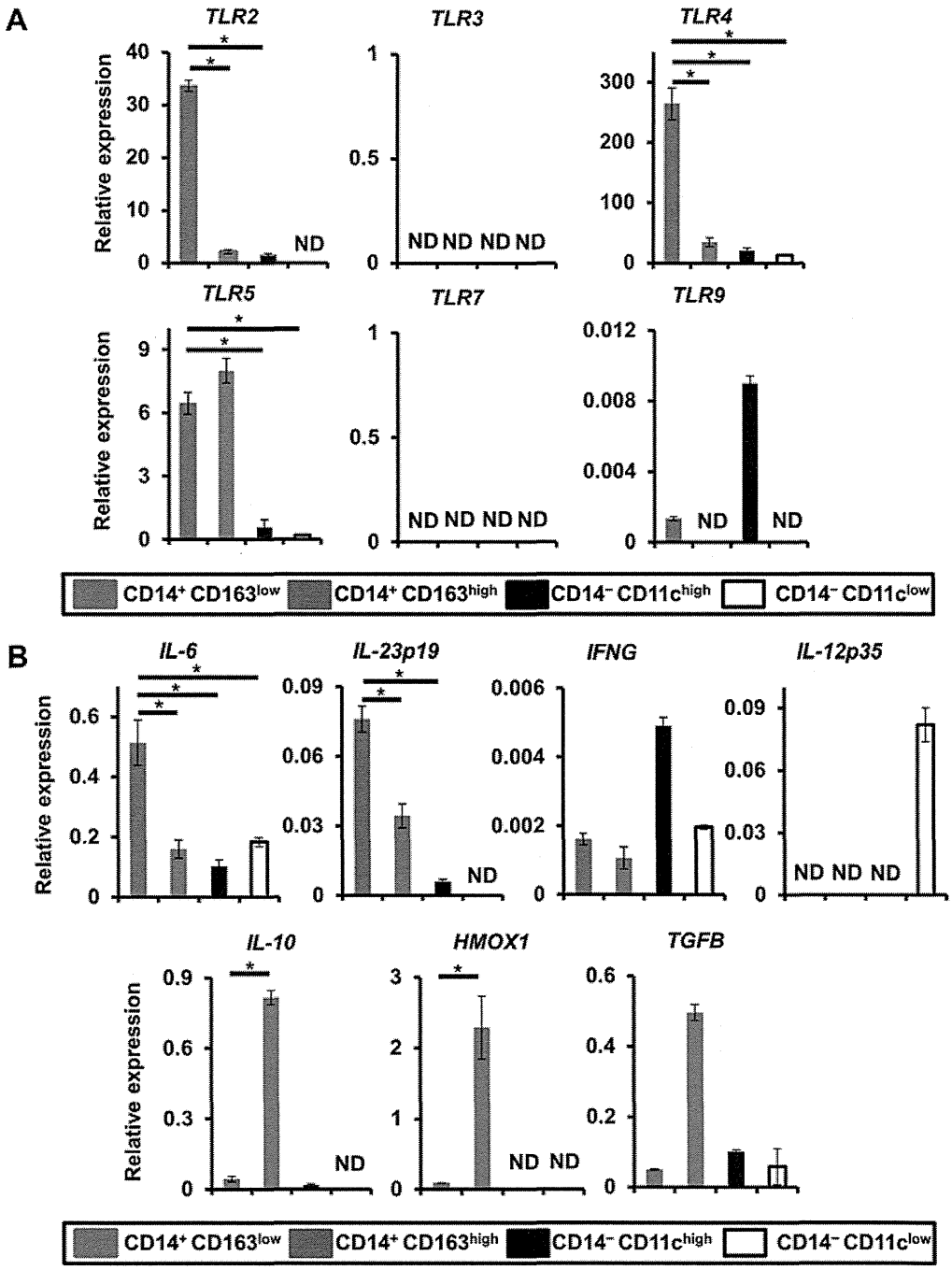

Figure 4. Various mRNA expression of LPC subsets. (*A*) Expression of *TLR2, TLR3, TLR4, TLR5, TLR7,* and *TLR9* in LPC subsets. (*B*) Expression of *IL-6, IL-23p19, IFNG, IL-12p35, IL-10, HMOX1,* and *TGFB* in LPC subsets. Results are mean ± SD from 5 independent experiments. ND, not detected. *$P < .01$.

$CD163^{high}$ cells were unique in their expression of anti-inflammatory genes.

Cytokine Production of LPC Subsets in Response to TLR Stimulation

To analyze the functions of these 4 subsets, we used enzyme-linked immunosorbent assay to assess their cytokine productions in response to TLR stimulation (Figure 5). Based on the *TLR* mRNA expression patterns, we used the TLR2 ligand FSL-1, the TLR4 ligand LPS, and the TLR5 ligand flagellin. High production of inflammatory cytokines, such as IL-6, IL-1β, and TNF-α, was observed in the $CD14^+$ $CD163^{low}$ cells, even without stimulation. $CD14^+$ $CD163^{low}$ cells produced increased amounts of IL-6, IL-1β, and TNF-α in response to LPS, but not in response to FSL-1 or flagellin. $CD14^+$ $CD163^{high}$ cells showed constitutive high production of IL-10, and $CD14^-$ $CD11c^{low}$ cells produced IL-12p70 in response to LPS and flagellin. These findings revealed differential patterns of cytokine production in the 4 LPC subsets, with the $CD14^+$ $CD163^{low}$ cells exhibiting LPS-induced inflammatory responses.

Induction of Th17 Cells by $CD14^+$ $CD163^{low}$ Cells

We next used the allogeneic mixed lymphocyte reaction technique to examine whether the 4 subsets induced Th1 or Th17 cell differentiation. After 5 days of co-culture, the IFN gamma and IL-17 productions of $CD4^+$ T cells were analyzed by intracellular cytokine staining (Figure 6*A*). We used monocyte-derived DCs as a control, which induced IFN-gamma–producing $CD4^+$ T cells (Th1 cells: 15.22% ± 7.19%), but not IL-17–producing $CD4^+$ T cells (Th17 cells: 0%). Naïve $CD4^+$ T cells co-cultured with $CD14^+$ $CD163^{low}$ cells produced high amounts of IL-17 (0.52% ± 0.17%) compared with those co-cultured with other subsets (Figure 6*B*), indicating that $CD14^+$ $CD163^{low}$ cells possess a high capacity

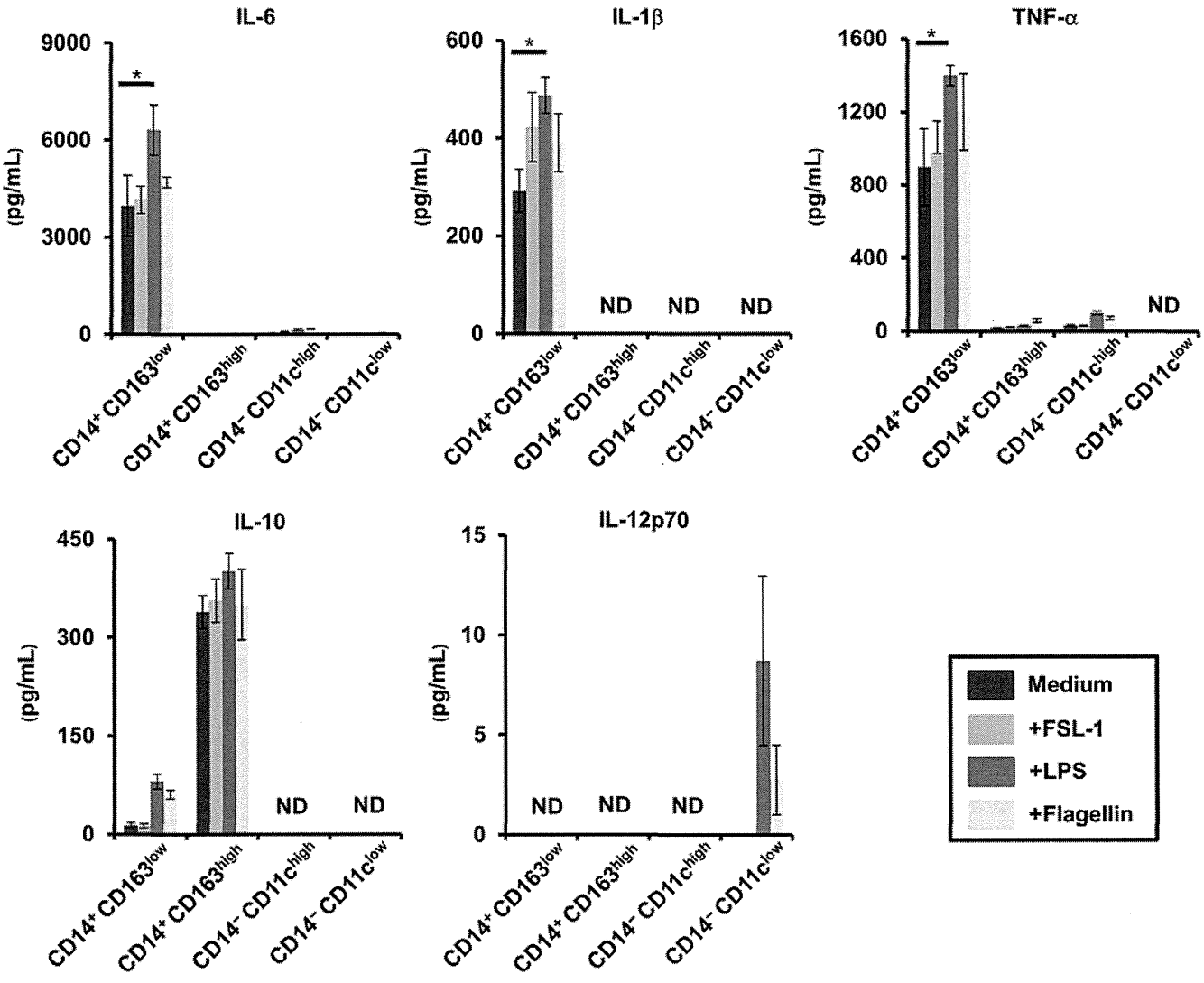

Figure 5. Cytokine production of LPC subsets. LPC subsets were analyzed for productions of IL-6, IL-1β TNF-α, IL-10, and IL-12p70 in response to FSL-1, LPS, or flagellin by enzyme-linked immunosorbent assay. Results are mean ± SD from 5 independent experiments. ND, not detected. *$P < .01$.

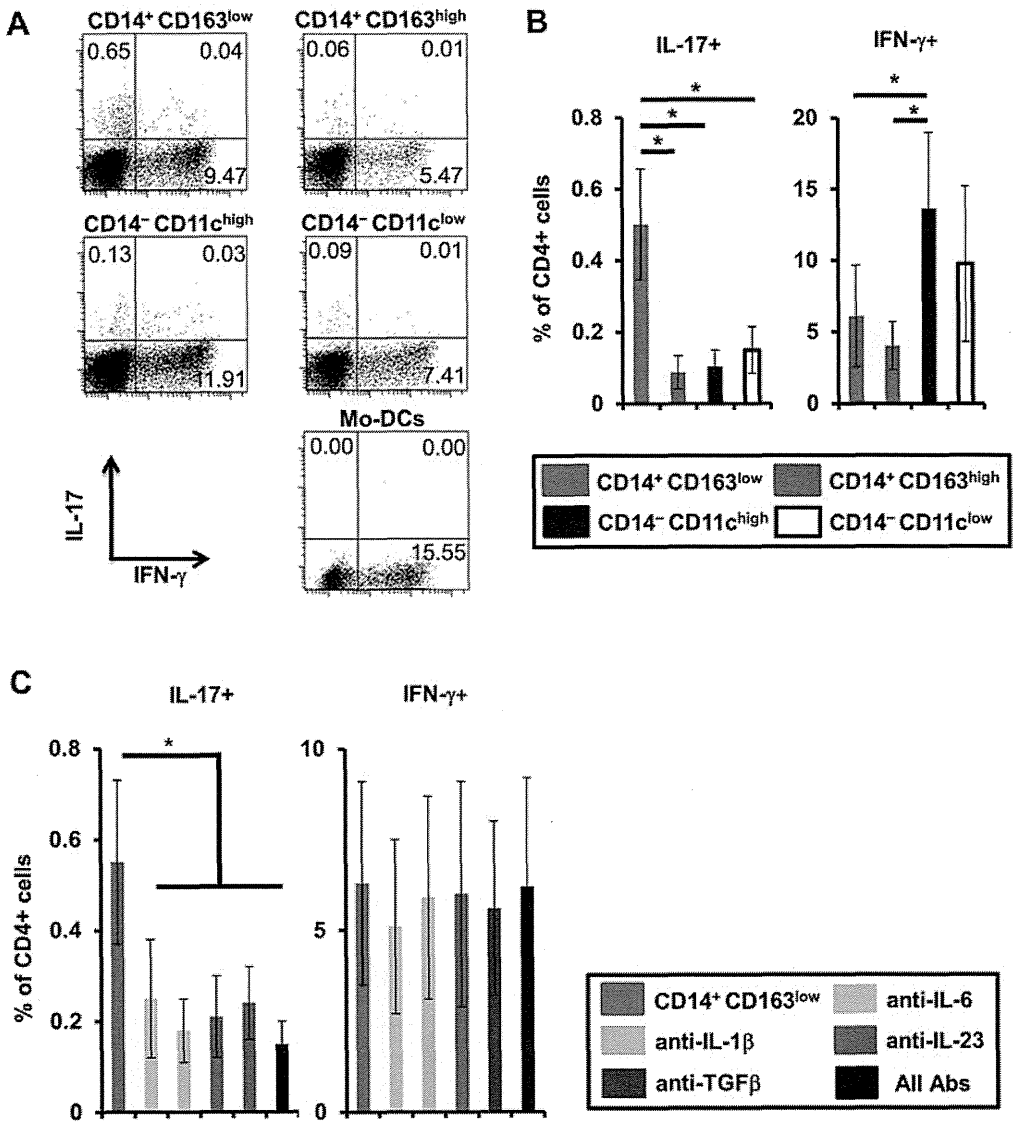

Figure 6. Functional properties of T-cell differentiation in LPC subsets. (*A*) Intracellular cytokine staining and flow cytometry performed to evaluate IFN gamma and IL-17 expression by naive T cells after 5 days of co-culture with allogeneic LPC subsets. Co-culture with monocyte-derived DCs was used as a control. Representative results of 8–14 independent experiments are shown. (*B*) Percentages of IL-17–producing cells and IFN gamma–producing cells among the $CD4^+$ cells after co-culture are shown. Results are mean ± SD from 7 independent experiments. *$P < .01$. (*C*) Intracellular cytokine (IL-17 and IFN gamma) staining of naive T cells after co-culture with allogeneic $CD14^+$ $CD163^{low}$ subsets in the presence or absence of the indicated blocking antibodies. Percentages of IL-17–producing cells and IFN gamma–producing cells among the $CD4^+$ cells are shown. Results are mean ± SD from 5 independent experiments. *$P < .01$.

to induce Th17 cells. Naïve $CD4^+$ T cells co-cultured with $CD14^-$ $CD11c^{high}$ cells produced high amounts of IFN gamma (13.78% ± 7.02%), indicating that $CD14^-$ $CD11c^{high}$ cells are DCs with a strong ability to induce Th1 cells. $CD14^-$ $CD11c^{low}$ cells induced moderate levels of Th1 cells (9.81% ± 6.75%) and very few, if any, Th17 cells (0.15% ± 0.06%). The $CD14^+$ $CD163^{high}$ cells showed the lowest ability to induce both Th1 and Th17 cells (4.07% ± 1.61% and 0.08% ± 0.04%, respectively). Overall, the 4 LPC subsets had differential activities for inducing Th1 and Th17 cells, with the $CD14^+$ $CD163^{low}$ cells highly inducing Th17 cells.

To analyze the impacts of IL-6, IL-1β, IL-23, and TGF-β on $CD14^+$ $CD163^{low}$ cell-dependent induction of Th17 cells, we blocked the effect of these cytokines using neutralizing antibodies. Th17 cell differentiation by $CD14^+$ $CD163^{low}$ cells was severely impaired in the presence of the blocking antibodies, and Th1 cell differentiation was not affected (Figure 6*C*).

Functional Analysis of $CD14^+$ $CD163^{low}$ Cells in CD

Because $CD14^+$ $CD163^{low}$ cells facilitated Th17 cell differentiation, we next analyzed these cells in CD patients. Among HLA-DR^{high} Lin^- cells, $CD14^+$ $CD163^{low}$ cells were observed almost equally in the noninflamed region of CD (CDn; 28.1% ± 7.1%) and the inflamed region of CD (CDi; 27.2% ± 7.8%) compared with normal colon from colon cancer patients (NC; 25.5 ± 9.4%) (Figure 7*A* and *B*). We also compared the cytokine gene expression of $CD14^+$ $CD163^{low}$ cells between NC, CDn, and CDi. $CD14^+$ $CD163^{low}$ cells in CDi expressed the highest levels of proinflammatory genes, such as *IL-6*, *IL-23p19*, *TNF*, and *IL-12p35*, as well as anti-inflammatory genes, such as *IL-10* and *TGFB*. $CD14^+$ $CD163^{low}$ cells in CDn also expressed higher *IL-6*, *IL-23p19*, and *TNF* and lower *IL-10* compared with those in NC. *TGFB* expression did not differ between $CD14^+$ $CD163^{low}$ cells in NC and CDn (Figure 7*C*). We next compared the abilities of

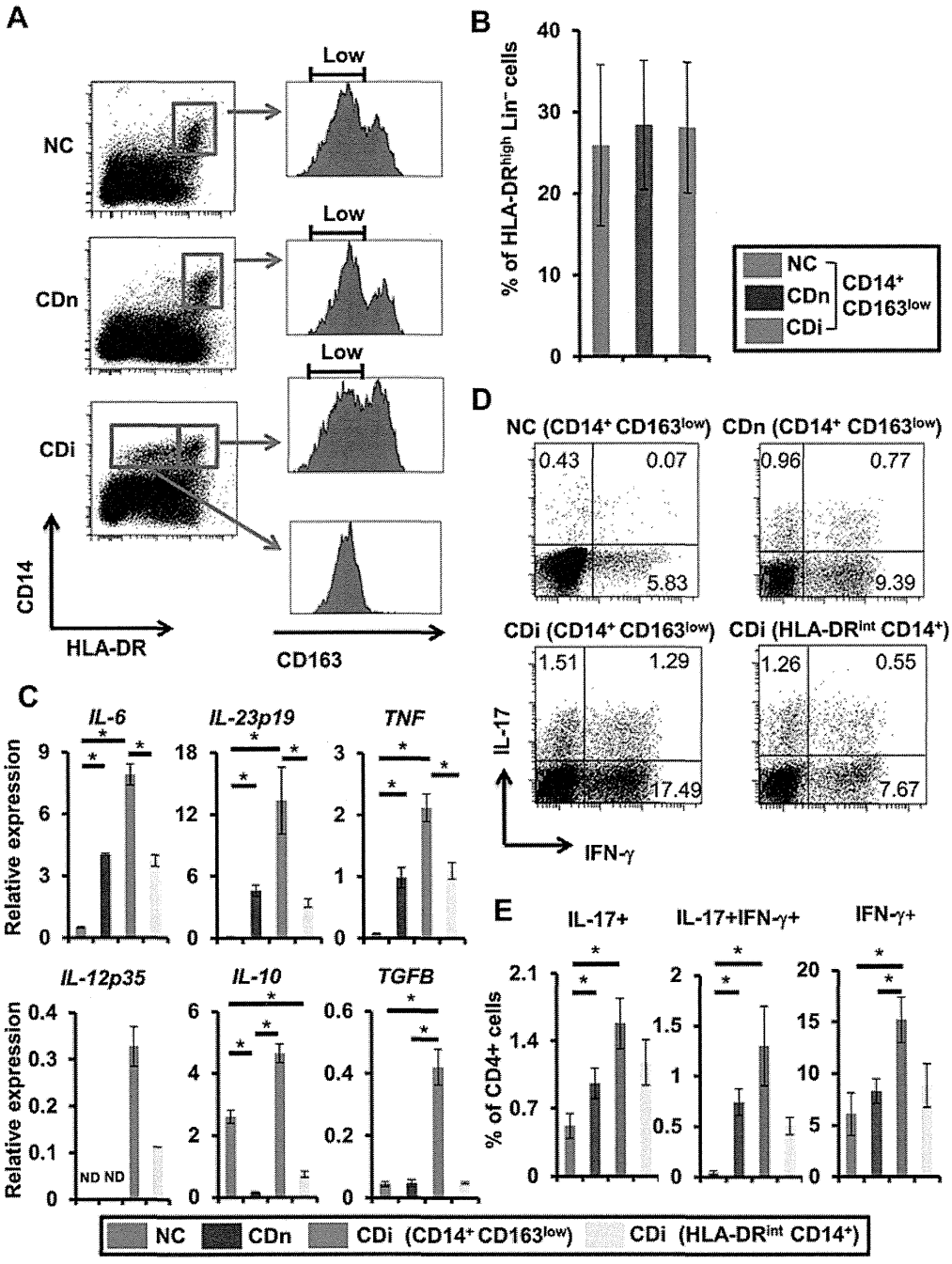

Figure 7. $CD14^+$ $CD163^{low}$ cells in Crohn's disease. (*A*) HLA-DR^{high} $CD14^+$ cells were gated and analyzed for CD163 expression in Lin^- cells from NC (n = 30), CDn (n = 22), or CDi (n = 19). Representative results are shown. (*B*) Percentages of $CD14^+$ $CD163^{low}$ cells from NC, CDn, and CDi in HLA-DR^{high} Lin^- cells are shown. (*C*) Expressions of various cytokine mRNAs in $CD14^+$ $CD163^{low}$ cells from NC, CDn, and CDi, and in HLA-DR^{int} $CD14^+$ cells from CDi. Results are mean ± SD from 5 independent experiments. ND, not detected. *$P <$ .01. (*D*) Intracellular cytokine (IL-17 and IFN gamma) staining of naive T cells after co-culture with $CD14^+$ $CD163^{low}$ cells from NC, CDn, and CDi, and with HLA-DR^{int} $CD14^+$ cells from CDi. Representative results of 5 independent experiments are shown. (*E*) Percentages of IL-17–producing cells, IL-17/IFN gamma double-producing cells, and IFN gamma–producing cells in $CD4^+$ cells after co-culture. Results are mean ± SD from 5 independent experiments. *$P <$ .01.

$CD14^+$ $CD163^{low}$ cells to induce Th1 and Th17 cell differentiation in NC, CDn, and CDi. As mentioned, $CD14^+$ $CD163^{low}$ cells in NC induced approximately 0.5% Th17 cells and few IFN gamma/IL-17 double-producing $CD4^+$ T cells (Th1/17 cells: 0.03% ± 0.01%) (Figure 7*D*). Compared with those in NC, $CD14^+$ $CD163^{low}$ cells in CDn induced similar numbers of Th1 cells (8.31% ± 1.18%), but larger numbers of Th17 (0.96% ± 0.16%) and Th1/17 cells (0.74% ± 0.13%). $CD14^+$ $CD163^{low}$ cells in CDi induced the largest numbers of Th17 cells (1.59% ± 0.26%), Th1/17 cells (1.3% ± 0.39%), and Th1 cells (15.23% ± 2.21%) (Figure 7*D* and *E*).

Interestingly, we found a unique population of HLA-DR intermediate (int) $CD14^+$ cells in CDi. This subset had expression patterns of surface molecules examined similar to $CD14^+$ $CD163^{low}$ cells (Supplementary Figure 3) and high expressions of *IL-6*, *IL-23p19*, and *TNF*, although these levels were lower than those of $CD14^+$ $CD163^{low}$ cells in CDi; these cells also exhibited low *IL-10* expression compared with those in NC (Figure 7*C*). HLA-DR^{int} $CD14^+$ cells induced high levels of Th17 cells (1.18% ± 0.24%) and Th1/17 cells (0.51% ± 0.09%), and moderate levels of Th1 cells (8.83% ± 2.1%) (Figure 7*D* and *E*).

Overall, we found that CD14$^+$ CD163^{low} cells in CDn exhibited high inflammatory cytokine production and strongly induced Th17 cells, and that this ability was further enhanced in CD14$^+$ CD163^{low} cells in CDi. In addition, a unique subset of HLA-DR^{int} CD14$^+$ cells in CDi showed strong ability to produce inflammatory cytokines and to induce Th17 cells.

Discussion

In this study, we characterized differential functions of 4 LPC subsets in the human colon. Within the HLA-DR^{high} Lin$^-$ population, CD14$^+$ CD163^{low} cells mediated Th17 cell differentiation. In CD patients, this subset had strong capacities for cytokine production and Th17 cell induction. It was recently reported that the CD14^{high} population in human ileal mucosa includes HLA-DR^{low} CD209^{low} CD163^{low}, HLA-DR^{high} CD209^{low} CD163^{low}, and HLA-DR^{high} CD209^{high} CD163^{high} cells.[28] In terms of the surface molecule expression patterns in these subsets, HLA-DR^{high} CD209^{low} CD163^{low} cells and HLA-DR^{high} CD209^{high} CD163^{high} cells in that report correspond approximately to the CD14$^+$ CD163^{low} cells and CD14$^+$ CD163^{high} cells, respectively, in the present study.

In mice, subsets of intestinal myeloid cells are already well characterized and are distinguished using combinations of surface markers, such as CD11b, CD11c, CD103, or CX3CR1.[16,21,24,29,35] In contrast, the appropriate surface markers for distinguishing myeloid cell subsets in humans remain unknown. In particular, CX3CR1 expression was hardly detected in human intestinal LPCs (unpublished results). In the present study, we found that LPCs in the HLA-DR^{high} Lin$^-$ population could be divided into CD14$^+$ CD163^{low}, CD14$^+$ CD163^{high}, CD14$^-$ CD11c^{high}, and CD14$^-$ CD11c^{low} subsets.

Mouse intestinal subpopulations, such as CX3CR1^{int} and CX3CR1^{high} cells, are present selectively in the intestine, not in MLN and spleen, under steady state.[25,29,36] Mouse CX3CR1^{int} cells, possessing macrophage-like and DC-like activities, highly express CD11c, major histocompatibility complex class II, and the co-stimulatory molecules CD86 and CD80. Consistent with murine CX3CR1^{int} cell expression of both macrophage (F4/80) and DC (DEC205) markers,[29,37,38] here we found that CD14$^+$ CD163^{low} cells expressed both macrophage- and DC-related markers. Gene expression profile analysis also indicates that CD14$^+$ CD163^{low} cells express genes that mediate macrophage- and DC-related functions. In addition, CD14$^+$ CD163^{low} cells exhibited macrophage-like morphology, like the case in intestinal CX3CR1$^+$ cells in mice.[17,28] These findings suggest that human CD14$^+$ CD163^{low} cells might be equivalent to CX3CR1^{int} cells in mice, which are derived from blood monocytes. CD14$^+$ CD163^{low} cells are monocyte-like lineage of cells that gain an ability of DC-related functions after migrating to the intestine. Similarly, a previous study suggests that CD14^{high} macrophages in normal and CD ileum are similar to CX3CR1^{int} cells in mice.[28] We found that CD14$^+$ CD163^{low} cells produced IL-1β, IL-6, TNF-α, and IL-23p19, as well as the anti-inflammatory cytokine IL-10. A recent study in mice suggests that CX3CR1^{int} cells produce not only IL-6 and TNF-α, but also low levels of IL-10.[23] In terms of cytokine production patterns, CD14$^+$ CD163^{low} cells in humans are similar to CX3CR1^{int} cells in mice, as found in the phenotypic analyses mentioned previously, further suggesting that CD14$^+$ CD163^{low} cells are a human counterpart to mouse CX3CR1^{int} cells.

There have been several reports analyzing human DC subsets. CD1c$^+$ cells in the intestinal lamina propria express higher levels of activation markers (CD40, CD83, CD86, HLA-DR) than those in blood and produce IL-23 at steady state.[39] The present study indicates that these CD1c$^+$ LPCs are further subdivided into CD14$^+$ CD163^{low}, CD14$^+$ CD163^{high} and CD14$^-$ CD11c^{high} cells, and that a main producer of IL-23 is CD14$^+$ CD163^{low} cells. Lung CD1c$^+$ DCs within the CD14$^-$ CD11c$^+$ population activate CD8$^+$ T cells with induction of CD103 expression via TGF-β.[40] Given the similar expression pattern of surface molecules, the lung CD1c$^+$ CD14$^-$ CD11c$^+$ DCs might correspond to the CD14$^-$ CD11c^{high} subset in the present study. CD141^{high} DCs, a functional homolog of mouse CD103$^+$ DCs, synthesize TNF-α, but not IL-12p70, in response to TLR3 stimulation.[41] CD141^{high} cells are present within the CD14$^-$ CD11c^{low} population, which produces IL-12p70 in response to LPS in the present study. In this regard, CD141$^-$ population within the CD14$^-$ CD11c^{low} population might be a IL-12p70 producer. Slan DCs expressing 6-sulfo LacNAc drive Th17/Th1 cell differentiation with production of IL-1β, IL-23, IL-12, and IL-6 in psoriasis patients.[42] The slan DCs do not express CD14 and CD163. CD14$^+$ CD163^{low} cells expressed 6-sulfo LacNAc, but had no production of IL-12p70. Given the differential profiles of surface marker expression and cytokine production, CD14$^+$ CD163^{low} cells are considered to be a distinct population from slan DCs observed in psoriasis patients.

Th17 cell-associated pro-inflammatory cytokines, such as IL-17 and IL-23, play key roles in several mouse autoimmune disease models and are thought to be involved in the pathogenesis of human immune disorders.[43–47] Several reports have identified innate immune cells driving Th17 differentiation. In mice, CX3CR1^{int} cells in the intestinal LP induce Th17 cells,[24,25] and TLR5$^+$ lamina propria DCs induce Th17 cell differentiation.[35] IRF4–dependent CD11b$^+$ DCs play a key role on Th17 induction.[48,49] Human ovarian tumor cells and tumor-associated antigen-presenting cells reportedly mediate Th17 cell generation at tumor sites.[50] Additionally, a human Th17-inducing inflammatory DC subset derived from blood monocytes was recently identified in synovial fluid of rheumatoid arthritis patients and inflammatory tumor ascites.[51] Human DCs inducing Th17 cell differentiation in the inflammatory condition have been identified; however, it remains unclear which human intestinal

LPC subsets are responsible for Th17 induction at steady state. In the present study, we showed that $CD14^+$ $CD163^{low}$ cells secreted IL-6 and IL-1β and differentiated naïve T cells into Th17 cells. $CD14^+$ $CD163^{low}$ cells are the main DCs that induce Th17-mediated immunity in the intestine.

Several recent studies have shown that IBD patients exhibit massive infiltration of Th17 cells in inflamed gastrointestinal mucosa, as well as increased serum IL-17 levels.[52,53] Polymorphisms in the gene encoding the IL-23 receptor are associated with CD.[8] In CD patients, TREM-1^+ macrophages are reportedly increased in intestinal mucosa and contribute to intestinal inflammation.[54] Spontaneous production of IL-1β and TNF-α is observed in $CD172a^+$ HLA-DR^+ cells, which accumulate into MLN and the intestinal mucosa of CD patients.[55] In the present study, we showed that the proportion of $CD14^+$ $CD163^{low}$ cells was not altered between NC and CDn. However, Th17 cell differentiation by $CD14^+$ $CD163^{low}$ cells was significantly higher in CDn than in NC. Abnormal activity of $CD14^+$ $CD163^{low}$ cells is evident, even in the non-inflamed intestine of CD patients. In addition, the $CD14^+$ $CD163^{low}$ cells in CDi had extremely enhanced ability to induce Th17 cells. These results indicated that $CD14^+$ $CD163^{low}$ cells might be involved in the progression of CD via Th17 immunity. Compared with NC and CDn, CDi involved huge numbers of HLA-DR^{int} $CD14^+$ cells. In this regard, HLA-DR^{int} $CD14^+$ cells might migrate from the bloodstream to the intestine in inflammatory environments, as has been reported for mouse $Ly6c^{high}$ $CX3CR1^{int}$ monocytes, which migrate into the intestine during intestinal inflammation.[28]

In conclusion, here we have identified $CD14^+$ $CD163^{low}$ cells as a subset that produces IL-6 and IL-1β, and can induce Th17 cells in human intestinal lamina propria. Further characterization of human $CD14^+$ $CD163^{low}$ cells showed them to be the putative equivalents of mouse $CX3CR1^{int}$ cells. Based on *TLR* expression and Th17 immunity, $CD14^+$ $CD163^{low}$ cells might play key roles in CD. Our findings suggest that $CD14^+$ $CD163^{low}$ cells could be a new diagnostic and therapeutic target for CD patients.

BASIC AND TRANSLATIONAL AT

Supplementary Material

Note: To access the supplementary material accompanying this article, visit the online version of *Gastroenterology* at www.gastrojournal.org, and at http://dx.doi.org/10.1053/j.gastro.2013.08.049.

References

1. Coombes JL, Powrie F. Dendritic cells in intestinal immune regulation. Nat Rev Immunol 2008;8:435-446.
2. Steinman RM, Hawiger D, Nussenzweig MC. Tolerogenic dendritic cells. Annu Rev Immunol 2003;21:685-711.
3. Strober W, Fuss I, Mannon P. The fundamental basis of inflammatory bowel disease. J Clin Invest 2007;117:514-521.
4. Xavier RJ, Podolsky DK. Unravelling the pathogenesis of inflammatory bowel disease. Nature 2007;448:427-434.
5. Neurath MF. IL-23: a master regulator in Crohn disease. Nat Med 2007;13:26-28.
6. Yen D, Cheung J, Scheerens H, et al. IL-23 is essential for T cell-mediated colitis and promotes inflammation via IL-17 and IL-6. J Clin Invest 2006;116:1310-1316.
7. Kobayashi T, Okamoto S, Hisamatsu T, et al. IL23 differentially regulates the Th1/Th17 balance in ulcerative colitis and Crohn's disease. Gut Microbes 2008;57:1682-1689.
8. Duerr RH, Taylor KD, Brant SR, et al. A genome-wide association study identifies IL23R as an inflammatory bowel disease gene. Science 2006;314:1461-1463.
9. Ogura Y, Bonen DK, Inohara N, et al. A frameshift mutation in NOD2 associated with susceptibility to Crohn's disease. Nature 2001; 411:603-606.
10. Hugot JP, Chamaillard M, Zouali H, et al. Association of NOD2 leucine-rich repeat variants with susceptibility to Crohn's disease. Nature 2001;411:599-603.
11. Khor B, Gardet A, Xavier RJ. Genetics and pathogenesis of inflammatory bowel disease. Nature 2011;474:307-317.
12. Barrett JC, Hansoul S, Nicolae DL, et al. Genome-wide association defines more than 30 distinct susceptibility loci for Crohn's disease. Nat Genet 2008;40:955-962.
13. Fisher SA, Tremelling M, Anderson CA, et al. Genetic determinants of ulcerative colitis include the ECM1 locus and five loci implicated in Crohn's disease. Nat Genet 2008;40:710-712.
14. Kayama H, Takeda K. Regulation of intestinal homeostasis by innate and adaptive immunity. Int Immunol 2012;24:673-680.
15. Varol C, Vallon-Eberhard A, Elinav E, et al. Intestinal lamina propria dendritic cell subsets have different origin and functions. Immunity 2009;31:502-512.
16. Schulz O, Jaensson E, Persson EK, et al. Intestinal CD103+, but not CX3CR1+, antigen sampling cells migrate in lymph and serve classical dendritic cell functions. J Exp Med 2009;206:3101-3114.
17. Bogunovic M, Ginhoux F, Helft J, et al. Origin of the lamina propria dendritic cell network. Immunity 2009;31:513-525.
18. Farache J, Koren I, Milo I, et al. Luminal bacteria recruit $CD103^+$ dendritic cells into the intestinal epithelium to sample bacterial antigens for presentation. Immunity 2013;21;38:581-595.
19. McDole JR, Wheeler LW, McDonald KG, et al. Goblet cells deliver luminal antigen to CD103+ dendritic cells in the small intestine. Nature 2012;483:345-349.
20. Jaensson E, Uronen-Hansson H, Pabst O, et al. Small intestinal CD103+ dendritic cells display unique functional properties that are conserved between mice and humans. J Exp Med 2008; 205:2139-2149.
21. Sun CM, Hall JA, Blank RB, et al. Small intestine lamina propria dendritic cells promote de novo generation of Foxp3 T reg cells via retinoic acid. J Exp Med 2007;204:1775-1785.
22. Johansson-Lindbom B, Svensson M, Pabst O, et al. Functional specialization of gut CD103+ dendritic cells in the regulation of tissue-selective T cell homing. J Exp Med 2005;202:1063-1073.
23. Weber B, Saurer L, Schenk M, et al. CX3CR1 defines functionally distinct intestinal mononuclear phagocyte subsets which maintain their respective functions during homeostatic and inflammatory conditions. Eur J Immunol 2011;41:773-779.
24. Denning TL, Wang YC, Patel SR, et al. Lamina propria macrophages and dendritic cells differentially induce regulatory and interleukin 17-producing T cell responses. Nat Immunol 2007;8:1086-1094.
25. **Atarashi K, Nishimura J**, Shima T, et al. ATP drives lamina propria TH17 cell differentiation. Nature 2008;455:808-812.
26. Zigmond E, Varol C, Farache J, et al. Ly6C hi monocytes in the inflamed colon give rise to proinflammatory effector cells and migratory antigen-presenting cells. Immunity 2012;37:1076-1090.
27. Rivollier A, He J, Kole A, et al. Inflammation switches the differentiation program of $Ly6C^{hi}$ monocytes from antiinflammatory macrophages to inflammatory dendritic cells in the colon. J Exp Med 2012; 209:139-155.
28. Bain CC, Scott CL, Uronen-Hansson H, et al. Resident and pro-inflammatory macrophages in the colon represent alternative

context-dependent fates of the same Ly6C^{hi} monocyte precursors. Mucosal Immunol 2013;6:498–510.
29. Kayama H, Ueda Y, Sawa Y, et al. Intestinal CX3C chemokine receptor 1 high (CX3CR1^{high}) myeloid cells prevent T-cell-dependent colitis. Proc Natl Acad Sci U S A 2012;109:5010–5015.
30. Hadis U, Wahl B, Schulz O, et al. Intestinal tolerance requires gut homing and expansion of FoxP3^{+} regulatory T cells in the lamina propria. Immunity 2011;34:237–246.
31. Smythies LE. Human intestinal macrophages display profound inflammatory anergy despite avid phagocytic and bacteriocidal activity. J Clin Invest 2005;115:66–75.
32. Smith PD, Smythies LE, Mosteller-Barnum M, et al. Intestinal macrophages lack CD14 and CD89 and consequently are down-regulated for LPS- and IgA-mediated activities. J Immunol 2001; 164:2651–2656.
33. Kamada N, Hisamatsu T, Okamoto S, et al. Unique CD14 intestinal macrophages contribute to the pathogenesis of Crohn disease via IL-23/IFN-gamma axis. J Clin Invest 2008;118:2269–2280.
34. Kamada N, Hisamatsu T, Honda H, et al. Human CD14+ macrophages in intestinal lamina propria exhibit potent antigen-presenting ability. J Immunol 2009;183:1724–1731.
35. Uematsu S, Fujimoto K, Jang MH, et al. Regulation of humoral and cellular gut immunity by lamina propria dendritic cells expressing Toll-like receptor 5. Nat Immunol 2008;9:769–776.
36. Diehl GE, Longman RS, Zhang JX, et al. Microbiota restricts trafficking of bacteria to mesenteric lymph nodes by CX3CR1^{hi} cells. Nature 2013;494:116–120.
37. Tamoutounour S, Henri S, Lelouard H, et al. CD64 distinguishes macrophages from dendritic cells in the gut and reveals the Th1-inducing role of mesenteric lymph node macrophages during colitis. Eur J Immunol 2012;42:1–17.
38. Niess JH, Adler G. Enteric flora expands gut lamina propria CX3CR1^{+} dendritic cells supporting inflammatory immune responses under normal and inflammatory conditions. J Immunol 2010; 184:2026–2037.
39. Dillon SM, Rogers LM, Howe R, et al. Human intestinal lamina propria CD1c+ dendritic cells display an activated phenotype at steady state and produce IL-23 in response to TLR7/8 stimulation. J Immunol 2010;184:6612–6621.
40. Yu CI, Becker C, Wang Y, et al. Human CD1c+ dendritic cells drive the differentiation of CD103+ CD8+ mucosal effector T cells via the cytokine TGF-beta. Immunity 2013;38:818–830.
41. Haniffa M, Shin A, Bigley V, et al. Human tissues contain CD141hi cross-presenting dendritic cells with functional homology to mouse CD103+ nonlymphoid dendritic cells. Immunity 2012;37:60–73.
42. Hansel A, Gunther C, Ingwersen J, et al. Human slan (6-sulfo LacNAc) dendritic cells are inflammatory dermal dendritic cells in psoriasis and drive strong TH17/TH1 T-cell responses. J Allergy Clin Immunol 2011;127:787–794.
43. Wong CK, Lit LC, Tam LS, et al. Hyperproduction of IL-23 and IL-17 in patients with systemic lupus erythematosus: implications for Th17-mediated inflammation in auto-immunity. Clin Immunol 2008; 127:385–393.
44. Ma HL, Liang S, Li J, et al. IL-22 is required for Th17 cell–mediated pathology in a mouse model of psoriasis-like skin inflammation. J Clin Invest 2008;118:597–607.
45. Komiyama Y, Nakae S, Matsuki T, et al. IL–17 Plays an important role in the development of experimental autoimmune encephalomyelitis. J Immunol 2006;177:566–573.
46. Chan JR, Blumenschein W, Murphy E, et al. IL-23 stimulates epidermal hyperplasia via TNF and IL-20R2-dependent mechanisms with implications for psoriasis pathogenesis. J Exp Med 2006; 203:2577–2587.
47. Kurosawa K, Hirose K, Sano H, et al. Increased Interleukin-17 production in patients with systemic sclerosis. Arthritis Rheum 2000; 43:2455–2463.
48. Schlitzer A, McGovern N, Teo P, et al. IRF4 Transcription factor-dependent CD11b+ dendritic cells in human and mouse control mucosal IL-17 cytokine responses. Immunity 2013;38:970–983.
49. Persson EK, Uronen-Hansson H, Semmrich M, et al. IRF4 transcription-factor dependent CD103+CD11b+ dendritic cells drive mucosal T helper 17 cell differentiation. Immunity 2013; 38:958–969.
50. Miyahara Y, Odunsi K, Chen W, et al. Generation and regulation of human CD4^{+} IL-17-producing T cells in ovarian cancer. Proc Natl Acad Sci U S A 2008;105:15505–15510.
51. Segura E, Touzot M, Bohineust A, et al. Human inflammatory dendritic cells induce th17 cell differentiation. Immunity 2013;38:336–348.
52. Veny M, Esteller M, Ricart E, et al. Late Crohn's disease patients present an increase in peripheral Th17 cells and cytokine production compared with early patients. Aliment Pharmacol Ther 2010; 31:561–572.
53. Fujino S, Andoh A, Bamba S, et al. Increased expression of interleukin 17 in inflammatory bowel disease. Gut 2003;52:65–70.
54. Schenk M, Bouchon A, Seibold F, et al. TREM-1-expressing intestinal macrophages crucially amplify chronic inflammation in experimental colitis and inflammatory bowel diseases. J Clin Invest 2007; 117:3097–3106.
55. Baba N, Van VQ, Wakahara K, et al. CD47 fusion protein targets CD172a+ cells in Crohn's disease and dampens the production of IL-1β and TNF. J Exp Med 2013;210:1251–1263.

Author names in bold designate shared co-first authorship.

Received March 29, 2013. Accepted August 22, 2013.

Reprint requests

Address requests for reprints to: Junichi Nishimura, MD, PhD, Department of Gastroenterological Surgery, Graduate School of Medicine, Osaka University, Yamadaoka 2-2, Suita City, Osaka 565-0871, Japan. e-mail: jnishimura@gesurg.med.osaka-u.ac.jp; fax: 81(0)6 6879 3259; or Kiyoshi Takeda, MD, PhD, Laboratory of Immune Regulation, Graduate School of Medicine, Osaka University, Yamadaoka 2-2, Suita City, Osaka 565-0871, Japan.
e-mail: ktakeda@ongene.med.osaka-u.ac.jp; fax: 81(0)6 6879 3989.

Conflicts of interest

The authors disclose no conflicts.

Supplementary Material

Antibodies for Flow Cytometry

The following antibodies were used: phycoerythrin (PE)-conjugated anti-CD3 (HIT3a; BD Biosciences), anti-CD19 (SJ25C1; BD Biosciences), anti-CD20 (2H7; BD Biosciences), anti-CD56 (B159; BD Biosciences), fluorescein isothiocyanate–conjugated anti-CD14 (MφP9; BD Biosciences), allophycocyanin-conjugated anti-CD11c (B-ly6; BD Biosciences), PE-Cy7–conjugated anti–HLA-DR (L243; Biolegend, San Diego, CA), peridinin chlorophyll protein complex-Cy5.5-conjugated anti-CD163 (GHI61; Biolegend), fluorescein isothiocyanate–conjugated anti-lineage (BD Biosciences), PE-Cy5–conjugated anti-CD86 (2331; BD Biosciences), anti-CD80 (L307.4; BD Biosciences), anti-CD83 (HB15e; BD Biosciences), anti-CD40 (5C3; BD Biosciences), PE-conjugated anti-CD64 (10.1; BD Biosciences), anti-CD103 (Ber-ACT8; Biolegend), anti-CD123 (7G3; BD Biosciences), anti-CD209 (DCN46; BD Biosciences), anti-CD11b (ICRF44; Biolegend), anti-CD141 (M80; Biolegend), anti-CD16 (3G8; BD Biosciences), anti-CD172a (SE5A5; Biolegend), anti-CD206 (15-2; Biolegend), anti-slan (DD-1; Miltenyi Biotec, Bergisch Gladbach, Germany), Brilliant Violet-conjugated anti-CD1c (L161; Biolegend), peridinin chlorophyll protein complex-Cy5.5-conjugated anti-CD4 (SK3; BD Biosciences), PE-conjugated anti-IL17A (N49-653; BD Biosciences), allophycocyanin-conjugated anti–IL-4 (MP4-25D2; BD Biosciences), and fluorescein isothiocyanate–conjugated anti–IFN-gamma (B27; BD Biosciences).

Intracellular Cytokine Analysis

$CD4^+$ T cells were stimulated for 4 hours in the presence of 5 μM calcium ionosphere (Sigma), 50 ng/mL phorbol myristate acetate (Sigma), and GolgiStop (BD Biosciences). Intracellular cytokine staining was subsequently performed with fixation and permeabilization buffers.

Preparation of Monocyte-Derived DCs

Peripheral $CD14^+$ monocytes were isolated from peripheral blood monocytes using CD14 microbeads (Miltenyi Biotec) following the manufacturer's instructions. For in vitro monocyte-derived DC differentiation, $CD14^+$ monocytes were cultured for 5 days in RPMI 1640 containing 10% fetal bovine serum, with 100 ng/mL recombinant human granulocyte macrophage colony-stimulating factor (Primmune, Kobe, Japan) and 100 U/mL recombinant human IL-4 (Primmune).

Microarray Analysis

Gene expression analysis using SurePrint G3 Human Gene Expression v2 8x60K Microarray (G4845A) (Agilent Technologies) was performed as one color experiments by the Dragon Genomics Center (TaKaRa Bio Inc., Shiga, Japan). Total RNA from $CD163^{high}$ ($CD14^+$ $CD163^{high}$), $CD163^{low}$ ($CD14^+$ $CD163^{low}$), DN ($CD14^-$ $CD11c^{low}$) and CD11c ($CD14^-$ $CD11c^{high}$) cells, which were derived from the sorted $HLA\text{-}DR^{high}$ Lin^- LPC subsets in noninvaded colonic tissue samples from individual colorectal cancer patients (n = 10) was extracted using RNeasy kit (Qiagen) following manufacturer's instructions. Twenty nanograms total RNA was reverse transcribed into double strand complementary DNAs by using an Ovation Pico WTA System V2 (NuGen) following manufacturer's protocol. Resulting complementary DNAs were subsequently used for in vitro transcription by DNA polymerase and labeled with cyanine-3 using a Genomic DNA Enzymatic Labeling Kit (Agilent Technologies) according to the manufacturer's protocol. After labeling, the labeled 2 μg of each complementary DNA sample was then hybridized on SurePrint G3 Human Gene Expression v2 8x60K Microarray at 65°C for 17 hours with rotation in the dark. Hybridization was performed using a Gene Expression Hybridization Kit (Agilent Technologies) following the manufacturer's instructions. After washing in GE washing buffer, slides were scanned with an Agilent Microarray Scanner G2505C. Feature extraction software (version 10.10.1.1) was used to convert images into gene expression data. Raw data were imported into GeneSpring GX 11.0 (Agilent Technologies) for database management and quality control. This normalized data without the threshold raw signal and the global normalization algorithm was used for identifying differentially expressed genes. Raw data have been accepted in Gene Expression Omnibus, a public repository for microarray data, aimed at storing Minimum Information About Microarray Experiments Access to data concerning this study is found under Gene Expression Omnibus experiment accession number GSE49066.

腫瘍内科，12(4)：394-400，2013

特集 治療効果の判定基準と臨床試験のendpoint

RECISTとirResponse Criteria 4) Mogamulizumabの効果判定*

和田 尚**
西塔拓郎**
長瀬博次**
土岐祐一郎**

Key Words：anti-CCR4 antibody, regulatory T cell, solid tumor, immune response, investigator initiated clinical trial

NY-ESO-1蛋白がんワクチン臨床試験で経験した1症例

筆者らは腫瘍免疫療法として，がん精巣抗原の一つであるNY-ESO-1をさまざまな形態で投与するがんワクチン臨床試験を行っている．NY-ESO-1全長蛋白にコレステロール抱合疎水化プルラン(CHP)をドラッグデリバリーシステムとして用い，その複合体CHP-NY-ESO-1を隔週で投与する臨床試験は2004年より行った[1)~3)]．進行食道がん・前立腺がん・悪性黒色腫患者13症例が参加した．ワクチン投与により，ほとんどの患者においてNY-ESO-1抗体価とNY-ESO-1特異的CD4，CD8 T細胞の反応が検出されるようになるか，あるいは上昇し，病変評価が可能であった食道がん症例6例中5例に腫瘍の一時退縮あるいは縮小などの臨床反応を認めた．食道がん症例E-1の経過を図に示す．頸部リンパ節転移腫瘤が，化学療法，放射線療法に抵抗性を示したためCHP-NY-ESO-1ワクチンを開始した．当初は，ワクチン投与にもかかわらず頸部リンパ節腫瘤は増大傾向を示し，ワクチン投与前の放射線化学療法で画像上消失していた食道がん原発部にも腫瘍の再増殖がみられるようになった(図1)．内視鏡検査では，食道内腔への腫瘍の浸潤が認められた(図2)．末梢血中の血清NY-ESO-1抗体価の早期よりの陽転化・増強に加えて，本人の強い希望によりワクチンを継続したところ，腫瘤は約4か月後に縮小傾向に転じ，内視鏡でも食道浸潤腫瘍の縮小が確認された．投与開始約1年後には画像上瘢痕と思われるまでになり，内視鏡検査では粘膜面に瘢痕が観察されるのみであった．これらの効果は半年以上持続した．この間，食道がんに対してワクチン以外の治療は行っていない．

腫瘍径の総和を図3に示す．ワクチン4回投与後には著明に増加し，明らかに進行(PD)と判定された．しかしその後は緩徐な減少を示し，結合組織様の像を示した期間は半年以上持続した．

化学療法では，投与開始直後より，あるいは2~3か月の期間を経ても腫瘍の増殖が観察される場合，その化学療法は無効である．効果判定基準も，数か月もの間の増殖期間を経て，その後に緩やかに腫瘍が縮小していくこの症例のような場合を想定していない．

がん免疫療法の特性

がん免疫療法が臨床効果を発揮するまでには時間がかかる．抗がん剤の化学的な腫瘍増殖抑

* Response criteria in mogamulizumab clinical trial.

** Hisashi WADA, M.D., Ph.D., Takuro SAITO, M.D., Hirotsugu NAGASE, M.D. & Yuichiro DOKI, M.D., Ph.D.: 大阪大学大学院医学系研究科外科学講座消化器外科学〔〒565-0871 大阪府吹田市山田丘2-2〕; Department of Gastroenterological Surgery, Osaka University, Graduate School of Medicine, Suita, Osaka 565-0871, JAPAN

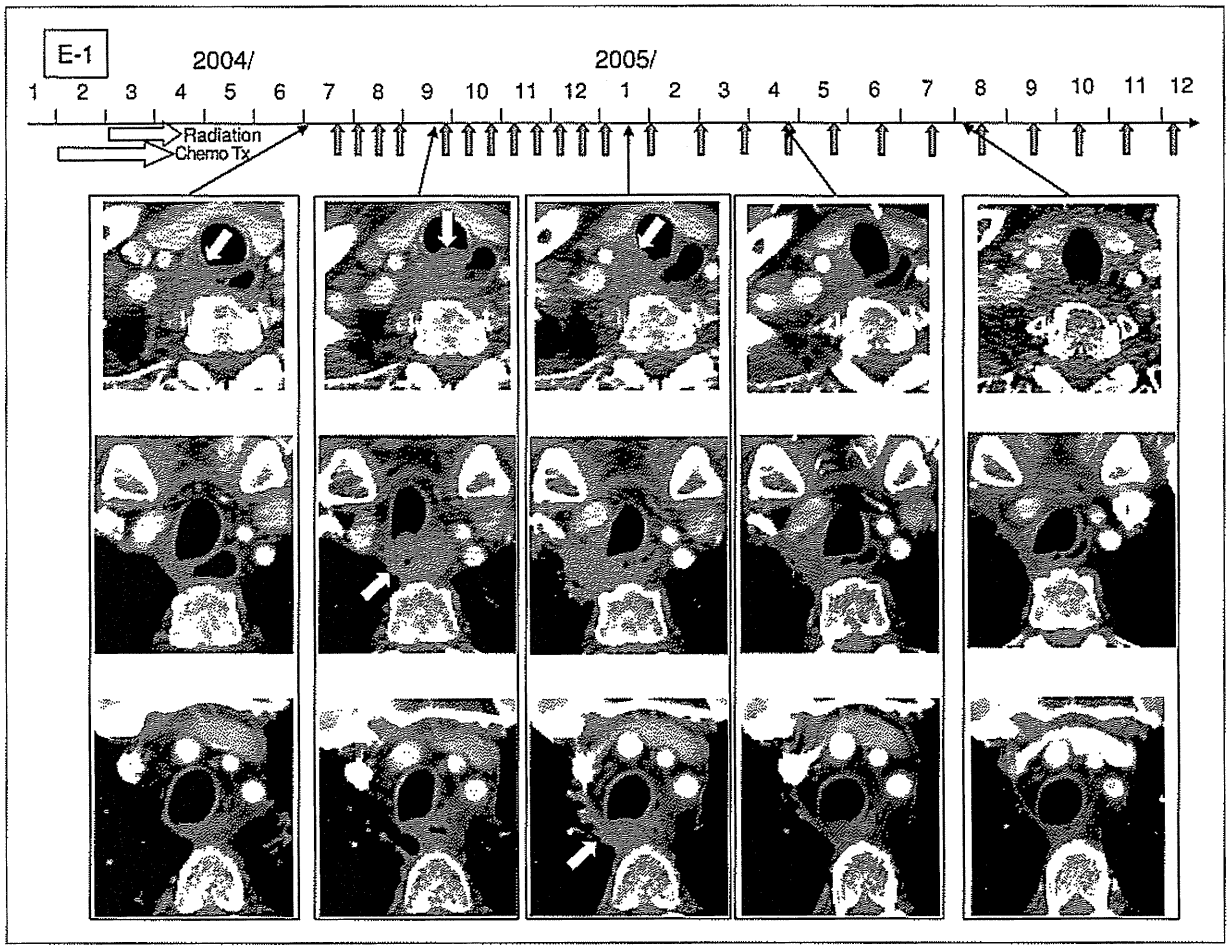

図1　CHP-NY-ESO-1がんワクチン臨床試験に参加した食道がん症例E-1の画像の経過
化学療法，放射線療法に抵抗性を示した頸部リンパ節転移腫瘤に対して2004年7月よりCHP-NY-ESO-1ワクチン(矢印)を開始した．頸部(上段)，胸腔上部2か所(中段，下段)のCT画像を経時的に示す．白矢印は腫瘤を示す．

制効果とは異なり，がん免疫の誘導・増強には時間が必要である．当初は抗腫瘍効果が腫瘍増殖に追いつかなくとも，やがて腫瘍増殖を凌駕し，腫瘍を縮小に導くと考えられている．

直接的に抗腫瘍効果を発揮するのはCD8陽性のリンパ球である細胞傷害性T細胞(CTL)である．能動免疫あるいは受動免疫などの免疫療法により体内に誘導あるいは投与されたがん細胞特異的反応性CTLは，抗原情報を持つ抗原提示細胞やがん細胞よりT細胞受容体を介したシグナルを受け取り，CTLの活性化とともに増殖し，反応性を増強する．抗腫瘍効果はこの数的・質的反応性の増強が，腫瘍増殖を凌駕するかにかかっている．

米国食品医薬品局(FDA)ガイダンス

免疫を介した抗腫瘍効果の特性は，2000年代初めから世界中で実施されるようになった腫瘍抗原の短鎖エピトープペプチドを用いたがんワクチン臨床試験を通じて認識されるようになった．これを受けて，米国食品医薬品局(FDA)は，“Clinical Considerations for Therapeutic Cancer Vaccines”として，企業向けにガイダンスを2009年9月に公表した．その中の臨床効果の判定に関する記述を抜粋・要約する[4]．

「背景；抗原投与から抗原提示などを経てリンパ球の活性化ののち，抗腫瘍効果を示すまでにはかなりの時間を必要とする．よって，がんワクチンの開発は，従来の細胞障害性薬剤などの開発とは異なる臨床試験デザインを考慮する必要がある．」

「後期臨床試験の考え方；免疫作用機序として，がんワクチンは投与後に免疫を誘導する期間を考慮する必要がある．たとえば，がんワクチン

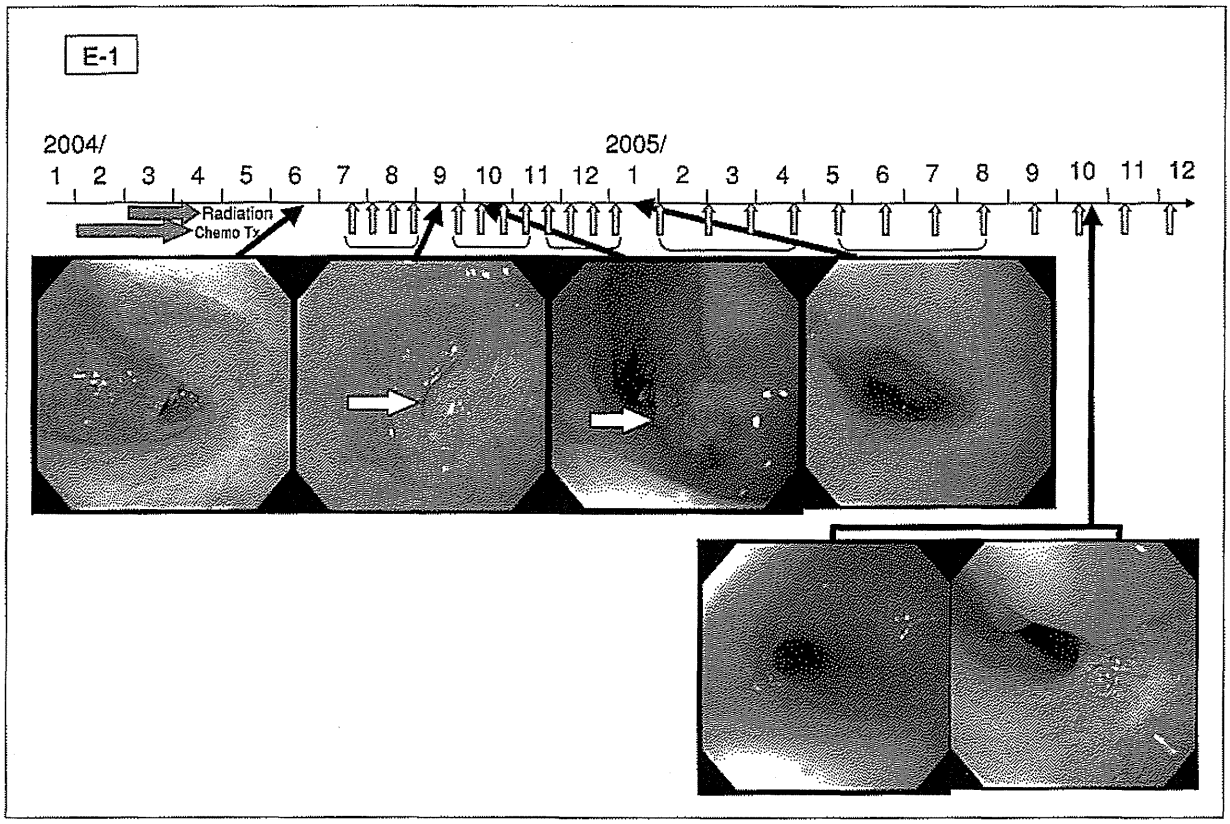

図2　E-1症例の上部消化管内視鏡写真
ワクチン投与後数か月後には食道内腔に浸潤する腫瘍(矢印)が観察されたが，やがて消褪し，瘢痕のみが残った．

治療初期には腫瘍は増大し続け，その後のワクチン治療継続によって遅れて起こる腫瘍退縮の場合，あるいは，がんワクチン治療初期の腫瘍増大，ワクチン治療継続によって起こる腫瘍退縮，そして再び増悪する場合，などである．このような遅発性の臨床効果が，非臨床データまたは早期臨床試験で示唆された場合，同じ臨床効果を期待して後期臨床試験を実施する際には，その薬剤に特化した臨床効果判定基準の設定など，個別のプロトコールで，特別な定義による統計解析をあらかじめ企図しておくことを推奨する．生存曲線のように，主目的の達成率を経時的に示す場合，試験初期ではがんワクチンは統計的にまったく効果を示さない場合があるかもしれない．そして，がんワクチンの臨床効果が現れる場合には，試験後期に曲線の分離が起こる可能性があると思われる．そのような場合，もしも旧来の方法のようにCoxモデルを適用すると，比例的ハザード仮定に従わず，統計学的仮説を実証するには多大な症例数が必要な事態となる．」

このガイダンスはがんワクチンに特化してのものではあるが，免疫を介する抗腫瘍療法全般に該当する記述であると考えられる．なお，2011年にも同様のガイダンスはFDAより公表されている[5]．

irRC

1．背　　景

FDAのガイダンスより遡り，腫瘍抗原エピトープペプチドによるがんワクチンが盛んであった2004年より，Cancer Vaccine Clinical Trial Working Groupを中心に臨床腫瘍医，免疫療法研究者そして規制の専門家たち約200人が集まり，がん患者に対する免疫療法の経験を報告するworkshopが数年間にわたり開かれた．何を目的として臨床試験を行うか，そのためにはどのようなデザインでどのような統計学的手法をとるか，今後の展開をどうすべきか，などが主に議論された[6]．

2．免疫療法に特有な臨床反応

このworkshopの中で，がんに対する免疫療法

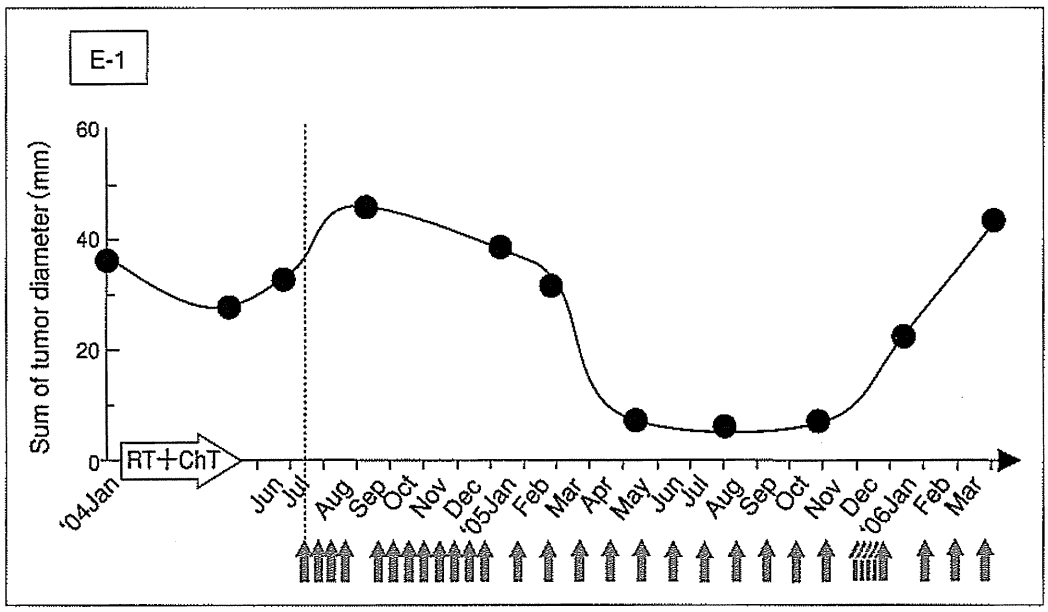

図3 E-1症例の腫瘍径の総和
ワクチン4回投与後においても増加を認めたが，その後は減少し，結合組織様の像を示した期間は半年以上持続した．

でしばしば見られる臨床反応を，有効な臨床効果としうるのかが議論され，次のように結論づけられた．①測定可能な抗腫瘍効果の発現には，抗がん剤などの細胞傷害性薬剤に比べて，長くかかる．②臨床効果はいわゆる「PD」ののちに現れる場合がある．③確実に「PD」でない限り免疫療法が中断されない方がいい場合がある．④(顕著な腫瘍縮小に際しての新規小病変の出現のような)臨床的に軽微な「PD」が許容されることを勧める．⑤持続する「SD」は抗腫瘍反応を示す可能性がある．このworkshopにはFDAからも担当者が参加しており，2009年のガイダンス公表へとつながった．

Wolchok博士らは，このworkshopの結論とFDAガイダンスを基本として，500例近い悪性黒色腫症例に対してipilimumabを投与した経験から，固形がんの免疫治療効果判定のためのガイドライン；Immune-Related Response Criteria(ir-RC)[7]を2009年11月に発表した．詳細は他編に譲るが，①実際の臨床効果が発現するまで時間的ずれが生じるので，PDが認められてもこれを容認し，レトロスペクティブに評価する，②治験薬投与開始後に新たな測定可能病変が認められても，腫瘍全体として縮小している場合は，治験薬の効果が示されていると考えられる，が要点である．

固形がんに対するmogamulizumab投与医師主導臨床治験

1．Mogamulizumab

Mogamulizumab(ポテリジオ®)は，協和発酵キリン(株)が開発したヒト化抗CCR4モノクローナル抗体KW-0761であり，脱フコシル化技術によりADCC活性を飛躍的に高めた抗体である．CCR4を発現する成人T細胞白血病リンパ腫(ATL)に対する治療薬剤として，2012年3月に厚労省より製造承認を受けた[8)9)]．

一方，制御性T細胞(Treg)は，CTLA-4やPD-1のような“immune checkpoint”分子と同様に，腫瘍免疫を抑制する細胞因子として広く知られている．TregはCD4CD25Foxp3陽性分画として認識されるが，その中でも$CD45RO^{+}Foxp3^{high}$の分画に免疫抑制機能を持つ活性化Tregが存在することが報告されている．この活性化分画ではCCR4が強発現している．マウスの系ではCD25抗体投与により，またCCR4アンタゴニストの投与でTregを除去することで腫瘍の退縮が起こる．ヒトでは，mogamulizumab治療を受けたATL患者体内でTregが除去されていることが確認されている[10)]．Treg除去を目的とした臨床試験はヒト化CD25抗体を用いすでに行われているが，一

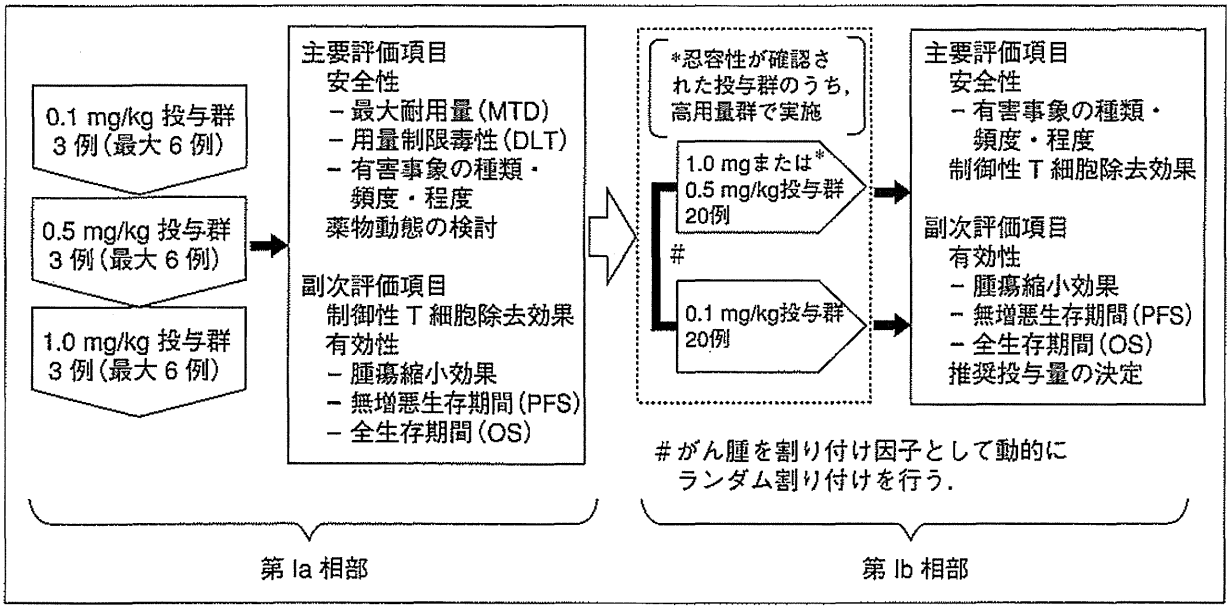

図 4　固形がんに対するmogamulizumab投与医師主導臨床治験デザイン

定の結論は出ていない．その中で今回のmogamulizumab投与は，Tregを直接標的とし，Treg除去を本来の目的とする新たながん免疫療法を提供しうる臨床試験である．

2．試験デザイン

今回の臨床治験では，標準治療抵抗性の進行または再発固形がん患者を対象として，mogamulizumabの反復静脈内投与によるTregの除去を介した腫瘍免疫増強による臨床効果を検討することを目的として，非盲検試験を実施する．このため対象疾患は固形がん症例とし，ATLとは異なりCCR4抗原を発現していないことを条件とした．第 Ia 相部で，主に安全性に基づき至適投与量を決定し，第 Ib 相部で，至適投与量でのTreg除去効果を評価する(図 4)．

第 Ia 相部では，mogamulizumab 0.1 mg/kg群 3 例(最大 6 例)，0.5 mg/kg群 3 例(最大 6 例)，そして1.0 mg/kg群 3 例(最大 6 例)について所定の用量の治験薬を週に 1 回 8 週連続で静脈内投与する．

第 Ib 相部では，第 Ia 相部において忍容性が確認された投与量の中で最高用量と0.1 mg/kgの 2 群を用いて各群第 Ia 相部の被験者とは別に各群20例(計40例)となるように投与する．投与は，週に 1 回の静脈内投与を 8 週連続で行う．ただし，第 Ia 相部において，忍容性が確認された投与量が0.1 mg/kgのみであった場合は，第 Ib 相部では，0.1 mg/kgの 1 用量を用いて20例となるように投与する．

8 回投与後治験薬の維持投与を可とする条件も設定した．

3．臨床効果評価方法

腫瘍縮小効果は，ir-RCを反映させるべく，RECIST Ver. 1.1に従った効果判定に加え，標的病変，非標的病変および新病変を以下のように定義した評価方法(以下，「RECISTの変法」という)を採用した．RECIST(ver. 1.1)と異なる箇所に下線を示す．

(1)標的病変

標的病変は，ベースラインにおいて最長径10 mm以上(リンパ節については短径で15 mm以上)の測定可能な病変とする．また，治験薬投与開始後に新たに認められた測定可能病変，および非標的病変が増大し最長径10 mm以上(リンパ節については短径で15 mm以上)の測定可能となった病変は標的病変に加えて評価する．標的病変数については制限を設けない．標的病変の評価は，最長径(リンパ節については短径)の和をベースラインと比較し，RECIST(ver. 1.1)の標的病変の判定基準にて評価する．

(2)非標的病変

非標的病変は，ベースラインにおいては，標的病変以外の病変とし，治験薬投与開始後においては，ベースラインで認められた非標的病変

のうち，治験薬投与開始後に最長径10 mm以上(リンパ節は短径で15 mm以上)に増大し，標的病変として評価されるものを除く病変とする．非標的病変の評価はRECIST(ver. 1.1)の非標的病変の判定基準にて評価する．

(3)新病変

新病変は，治験薬投与開始後に認められた骨病変，軟膜病変，腹水，胸水/心膜液，皮膚リンパ管炎，肺リンパ管炎，画像検査で確認できない腹部腫瘤，嚢胞性病変，髄膜炎等の測定不能病変とする．最長径10 mm未満(リンパ節は短径で15 mm未満)の病変に関しては新病変として取り扱わない．また，治験薬投与開始後に新たに認められた最長径10 mm以上(リンパ節については短径で15 mm以上)の測定可能病変は，標的病変として評価することから新病変として取り扱わない．

(4)PD判定時期

12週目までにPDの判定基準を満たした場合でも，12週以降も治験を継続している場合は，その時点ではPDとして取り扱わない．RECISTの変法のPD確認日は，12週を超えて最初にPDが確認された日とする．ただし，12週を超えた最初の評価がPDであった場合，その時点から評価時期を遡って初めにPDとなった日付をPD確認日とし，遡った評価時期にPDがない場合には12週を超えて最初にPDとなった日をPD確認日として解析する．病状の急激な増悪等の理由により，必要な検査ができなかった場合は，臨床上増悪が明らかと判断された日をもってPD確認日とする．PDが確認される前に死亡した症例については，死亡理由のいかんを問わず，治験実施計画書に定められた直近の来院日をPD確認日とみなす．

おわりに

上記のように，われわれはmogamulizumab投与医師主導治験において，RECISTの変法を使用するが，「PD」後の腫瘍縮小は，先に示したわれわれが実際に経験した症例からも，また望ましい反応であるという意味からも受け入れられやすい修正点である．一方で新規病変を「PD」に含めない点については，まだアレルギーを示す臨床医も多い．その意味でもir-RCを免疫療法に応用するに際して，都合のいい扱い方をしてはならない．本邦においても新規免疫療法が種々のがん種に対して投与されようとしている．臨床反応の経験を積み重ねることにより，ir-RCの再評価，再認識が可能であろう．

文　献

1) Wada H, Sato E, Uenaka A, et al. Analysis of peripheral and local anti-tumor immune response in esophageal cancer patients after NY-ESO-1 protein vaccination. Int J Cancer 2008 ; 123 : 2362.
2) Kawabata R, Wada H, Isobe M, et al. Antibody response against NY-ESO-1 in CHP-NY-ESO-1 vaccinated patients. Int J Cancer 2007 ; 120 : 2178.
3) Wada H, Uenaka A, Isobe M, et al. T cell immunomonitoring and tumor responses in patients immunized with a complex of cholesterol-bearing hydrophobized pullulan (CHP) and NY-ESO-1 protein. Cancer Immun 2007 ; 7 : 9.
4) Available from : URL : http://www.fda.gov/BiologicsBloodVaccines/GuidanceComplianceRegulatoryInformation/Guidances/Vaccines/ucm182443.htm.
5) Available from : URL : http://www.fda.gov/downloads/biologicsbloodvaccines/guidancecomplianceregulatoryinformation/guidances/vaccines/ucm278673.pdf#search='FDA+guidance+2011+cancer+vaccine'.
6) Hoos A, Parmiani G, Hege K, et al. A clinical development paradigm for cancer vaccines and related biologics. J Immunother 2007 ; 30 : 1.
7) Wolchok JD, Hoos A, O'Day S, et al. Guidelines for the evaluation of immune therapy activity in solid tumors : immune-related response criteria. Clin Cancer Res 2009 ; 15 : 7412.
8) Ishida T, Joh T, Uike N, et al. Defucosylated anti-CCR4 monoclonal antibody (KW-0761) for relapsed adult T-cell leukemia-lymphoma : a multicenter phase II study. J Clin Oncol 2012 ; 30 : 837.
9) Ishida T, Ueda R. Antibody therapy for Adult T-cell leukemia-lymphoma. Int J Hematol 2011 ; 94 : 443.
10) Ishida T, Ito A, Sato F, et al. Stevens-Johnson Syn-

drome associated with mogamulizumab treatment of adult T-cell leukemia/lymphoma. Cancer Sci 2013；104：647.

＊ ＊ ＊